Mass and Energy Flows into the Ionosphere from the Ring Current-Plasmasphere Interface

Janet Kozyra

“Physics made simple”

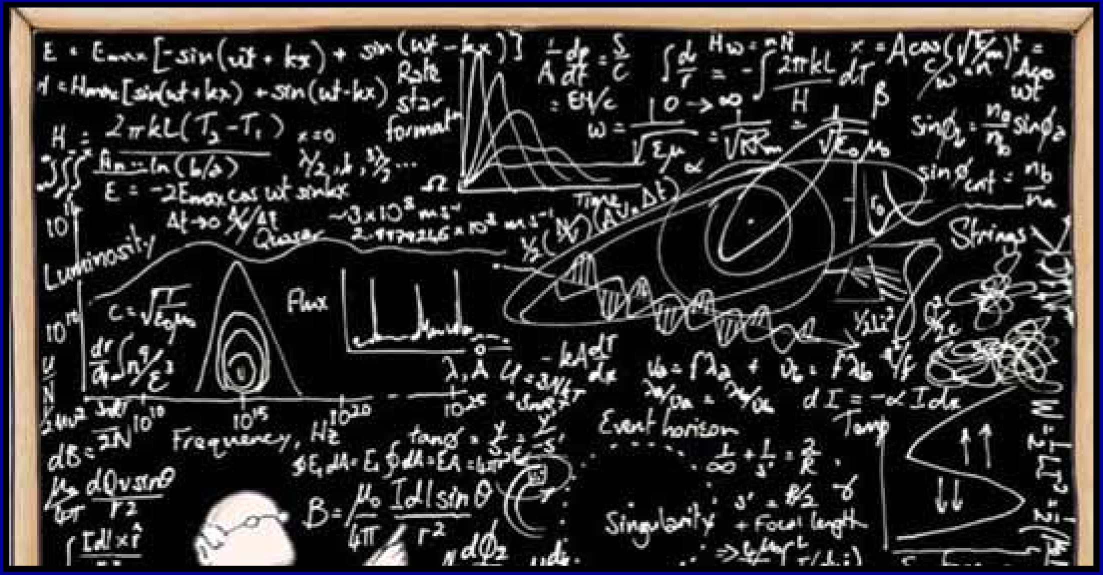

http://www.nearingzero.net/

GEM/CEDAR Tutorial
Santa Fe, New Mexico 2005

Ring current is the source of heat and particle fluxes in regions of overlap with the geocorona & plasmasphere

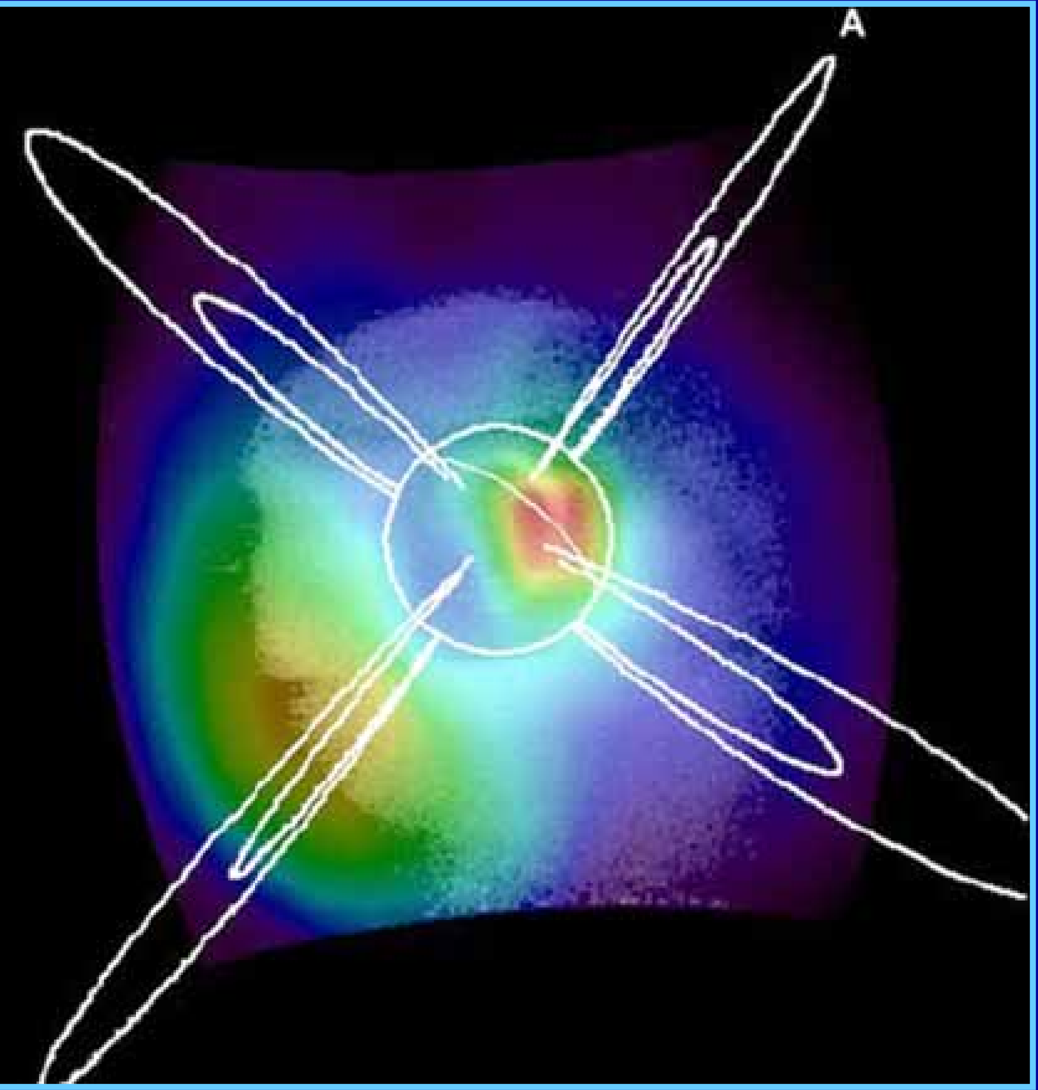

Burch et al., GRL, 2001

- What processes produce heat fluxes and create ion precipitation in the inner magnetosphere
- What are the impacts to the underlying ionosphere/ atmosphere?
- What are the major unknowns? New science questions?

Details of the Coupling Processes

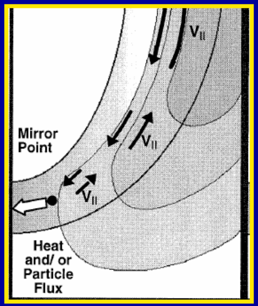

- Heat Flux: Coulomb collisions between ring current ions and plasmaspheric electrons

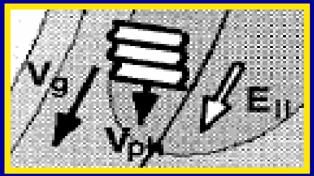

- Ion Precipitation:
  - —Anisotropic (in PA) ring current ions drive EMIC wave growth. EMIC waves scatter resonant ions into the loss cone

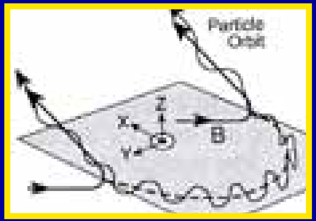

  - —Stretched magnetic fields scatter ions with gyroradius larger than field-line curvature into the loss cone.

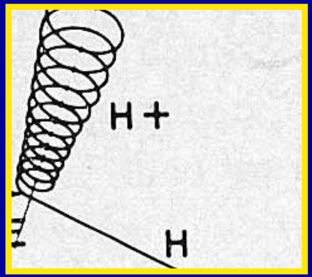

- Neutral Atom Precipitation: Ring current ions charge exchange with the geocorona to produce ENA, which sprays out in all directions. Some fraction encounters the atmosphere.

Coulomb collisions result in minor loss to the ring current (<10%) but major ionospheric effects

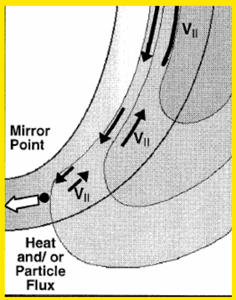

Handbook on Geophysics & Space Environment, 1985

QuickTime™ and a TIFF (LZW) decompressor are needed to see this picture.

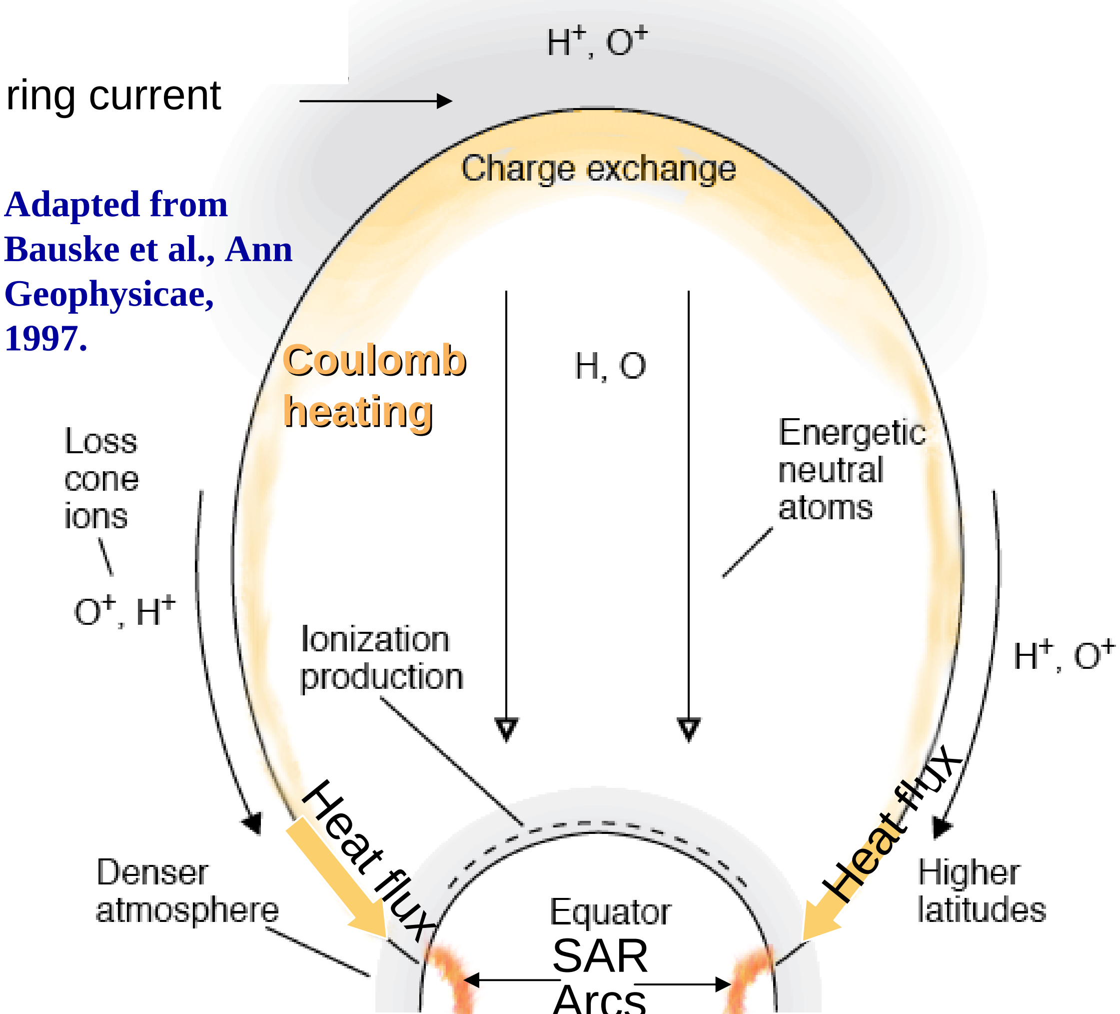

Adapted from Bauske et al., Ann Geophysicae, 1997.

- Inelastic collision. Ring current ion interacts with combined electric fields of plasma particles out to the Debye shielding distance $r_A = \lambda_D$
- Changes in energy of the incident ion appear as a series of incremental energy losses as the ion slows down but is not significantly deflected from its original path.
- Collisions with thermal electrons are more frequent than with thermal ions because comparable velocity keeps them in close proximity [Spitzer, 1956]

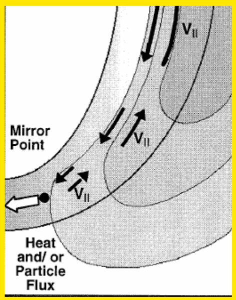

Interaction of Different Ions with the Plasmasphere [c.f., Kozyra et al., Rev of Geophys., 1997]

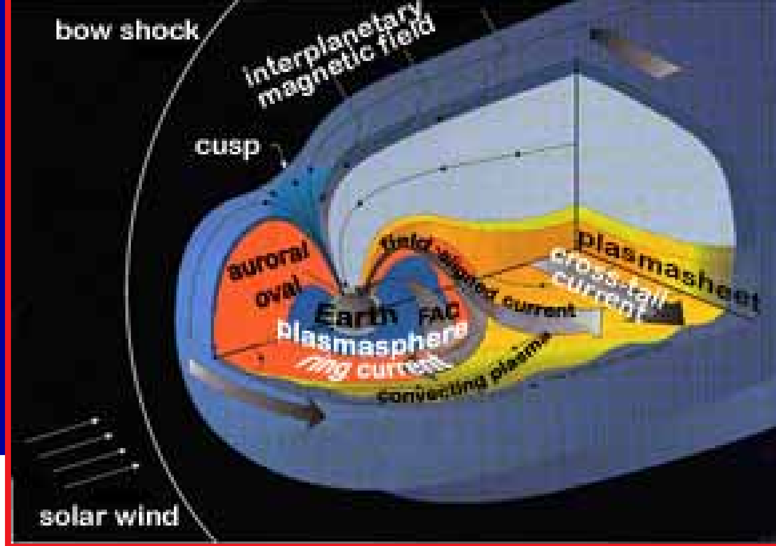

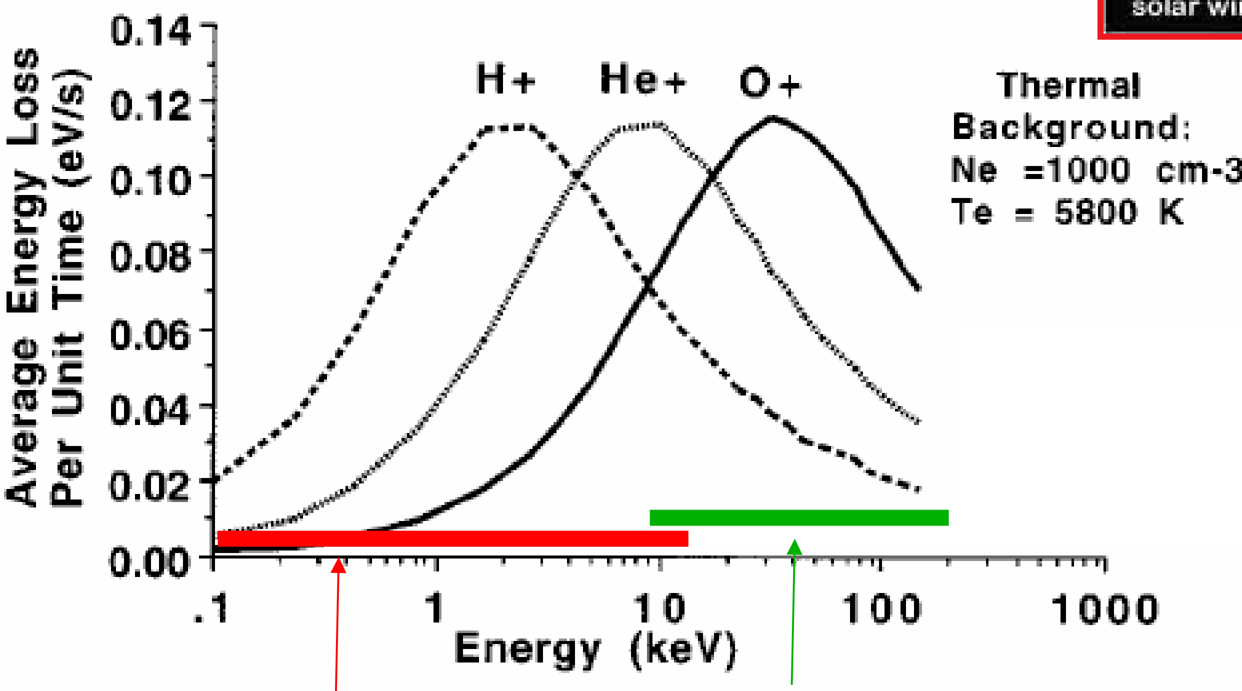

energy range of superstorm soft ions

energy range of ring current ions

Note: A population of >10 keV H^+ ions overlapping the plasmasphere (as seen in superstorms) could also supply significant magnetospheric heat flux

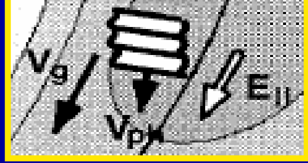

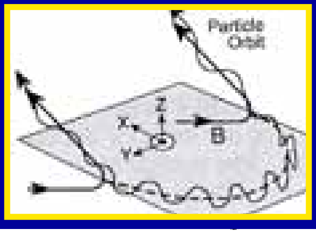

Ions enter the loss cone through interactions with plasma waves or scattering in stretched magnetic fields

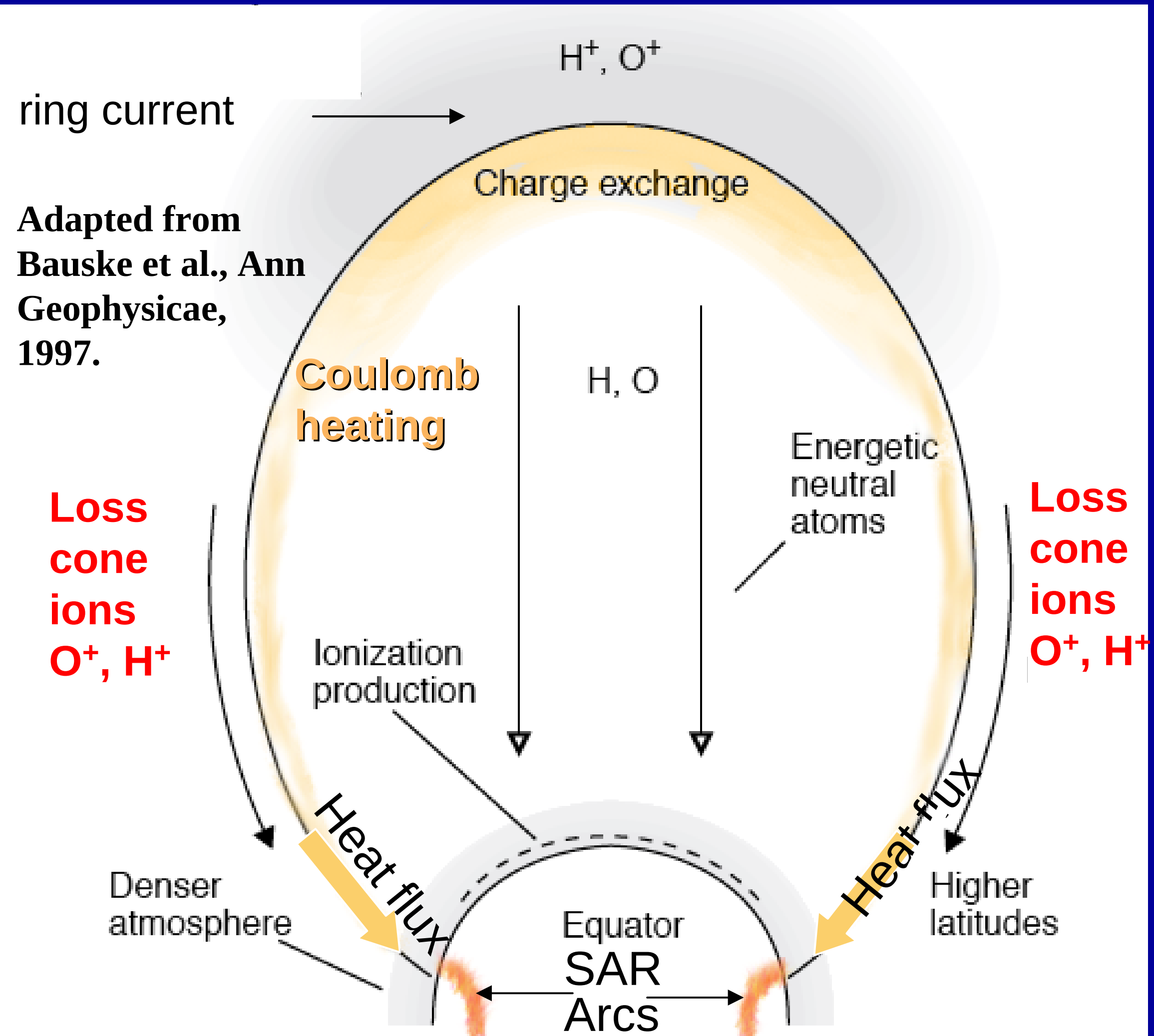

Adapted from Bauske et al., Ann Geophysicae, 1997.

Basic Facts About Wave-Particle Interactions

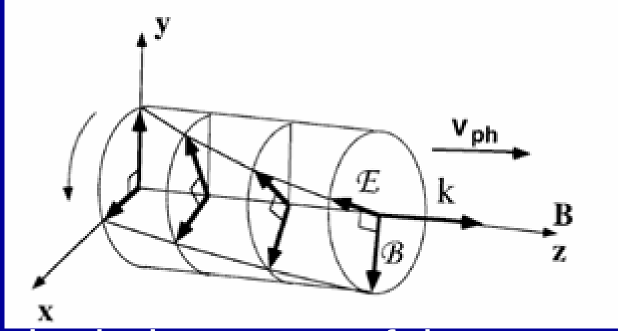

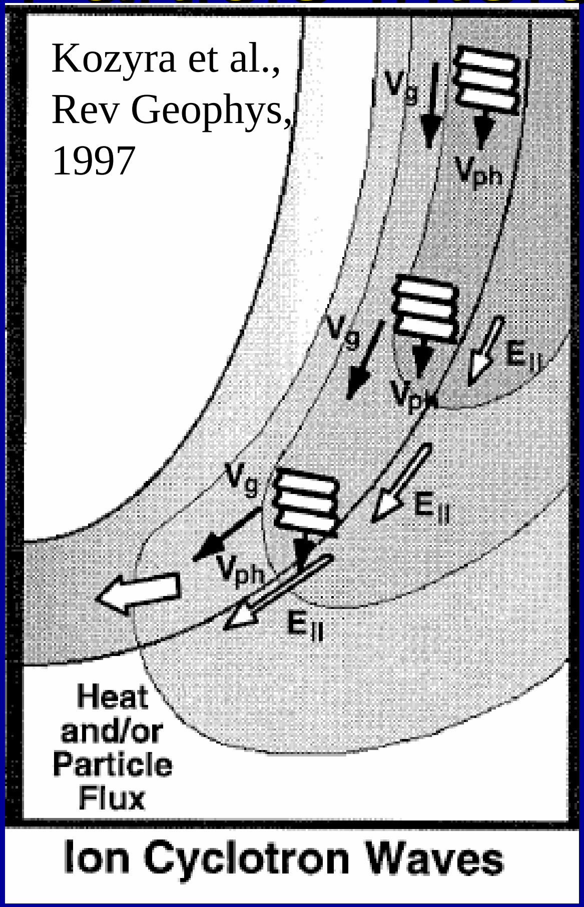

Cyclotron Resonance: When both the sense of the rotation and rotation frequency match for both wave and particle, the particle will essentially see a constant wave field. The particle can exchange energy with the wave E field or be deflected in pitch angle by the wave B field.

- Damping: particle gain energy from waves.
- Growth: waves gain energy from particles

Landau Damping: EM waves acquire a parallel E field when the wave vector makes a finite angle with the dc magnetic field. Particles traveling slightly slower (faster) than the wave will be accelerated (decelerated).

SAR arc theory: Ring current ions amplify ICW waves & scatter into loss cone. Ion cyclotron waves damped by plasmaspheric electrons which gain parallel velocity. Heat (low energy electron) flux into ionosphere powers SAR arcs [Cornwall et al., 1971].

Problem: Ion cyclotron wave not observed with sufficient frequency, spatial extent, or duration. Still open question.

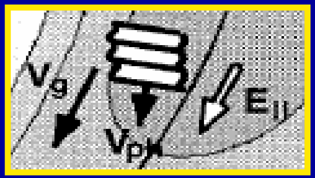

AMPTE/CCE Occurrence rate of ion cyclotron waves peaks near 10% at L values > 6 in prenoon to dusk sector.

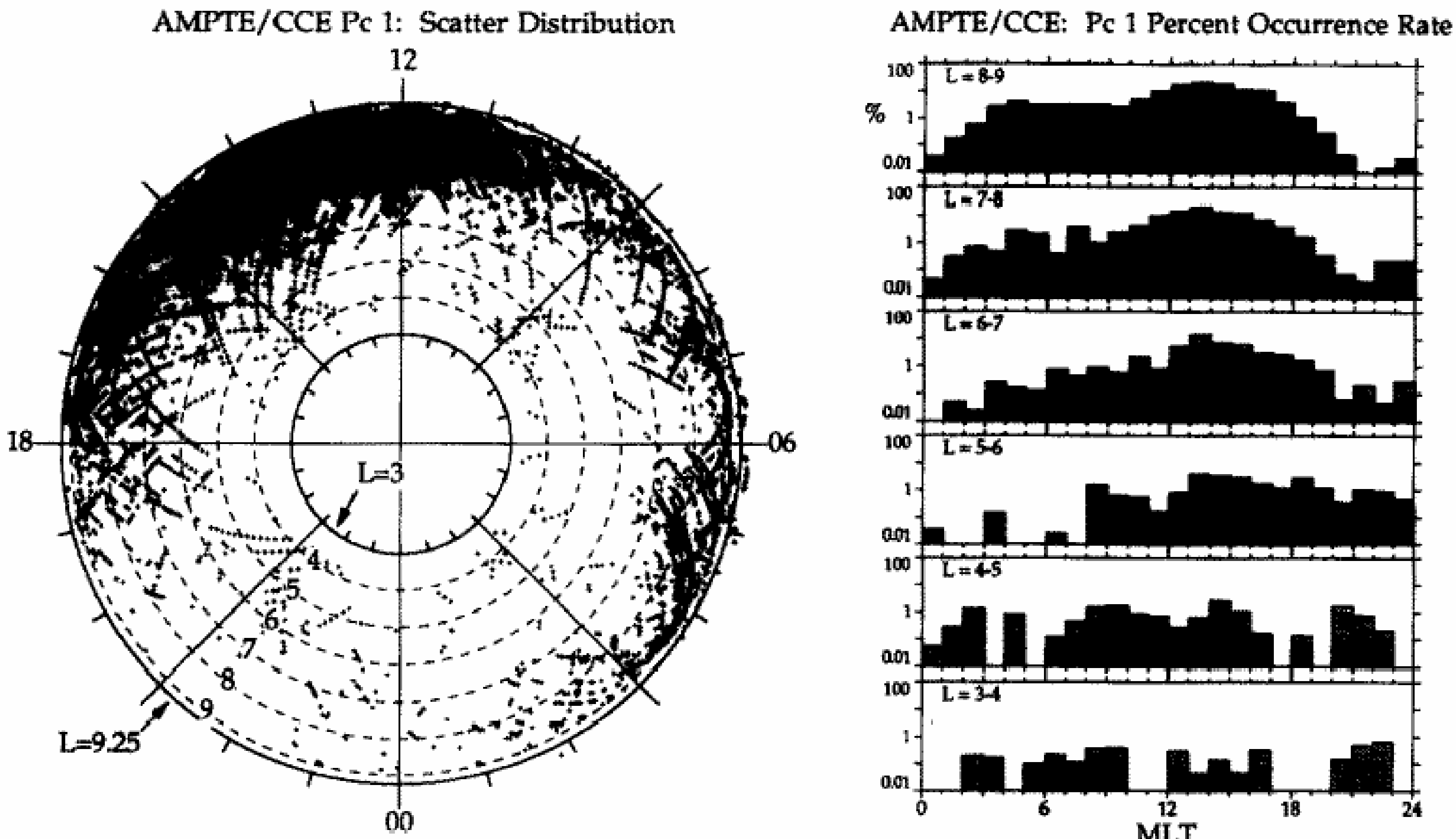

Anderson et al., Adv. Space Res., 1996

Fig. 1. Scatter plot (left) and normalized occurrence rate (right) of EMIC wave events observed by AMPTE/CCE in an *L*-MLT projection /25/.

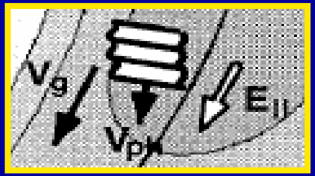

CRRES statistics for ion cyclotron waves in agreement with AMPTE/CCE - mostly outside plasmapause

Normalized He+ cyclotron frequency

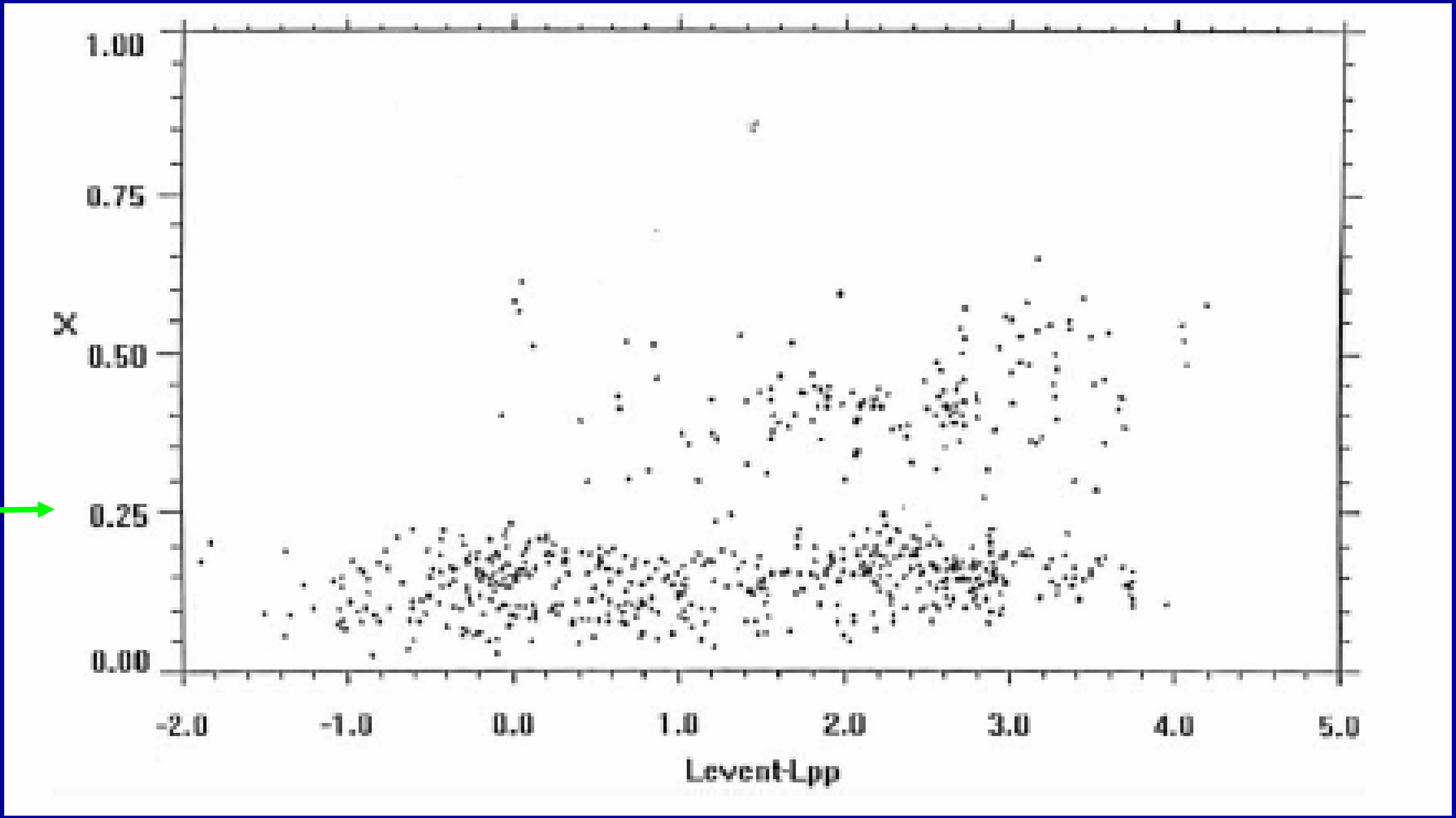

Waves in frequency band above He+ cyclotron frequency only occur outside the plasmasphere. [Fraser and Nguyen, JASTP, 2001]

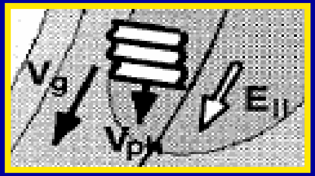

CRRES statistics for ion cyclotron waves in agreement with AMPTE/CCE - highest occurrence in dusk bulge region

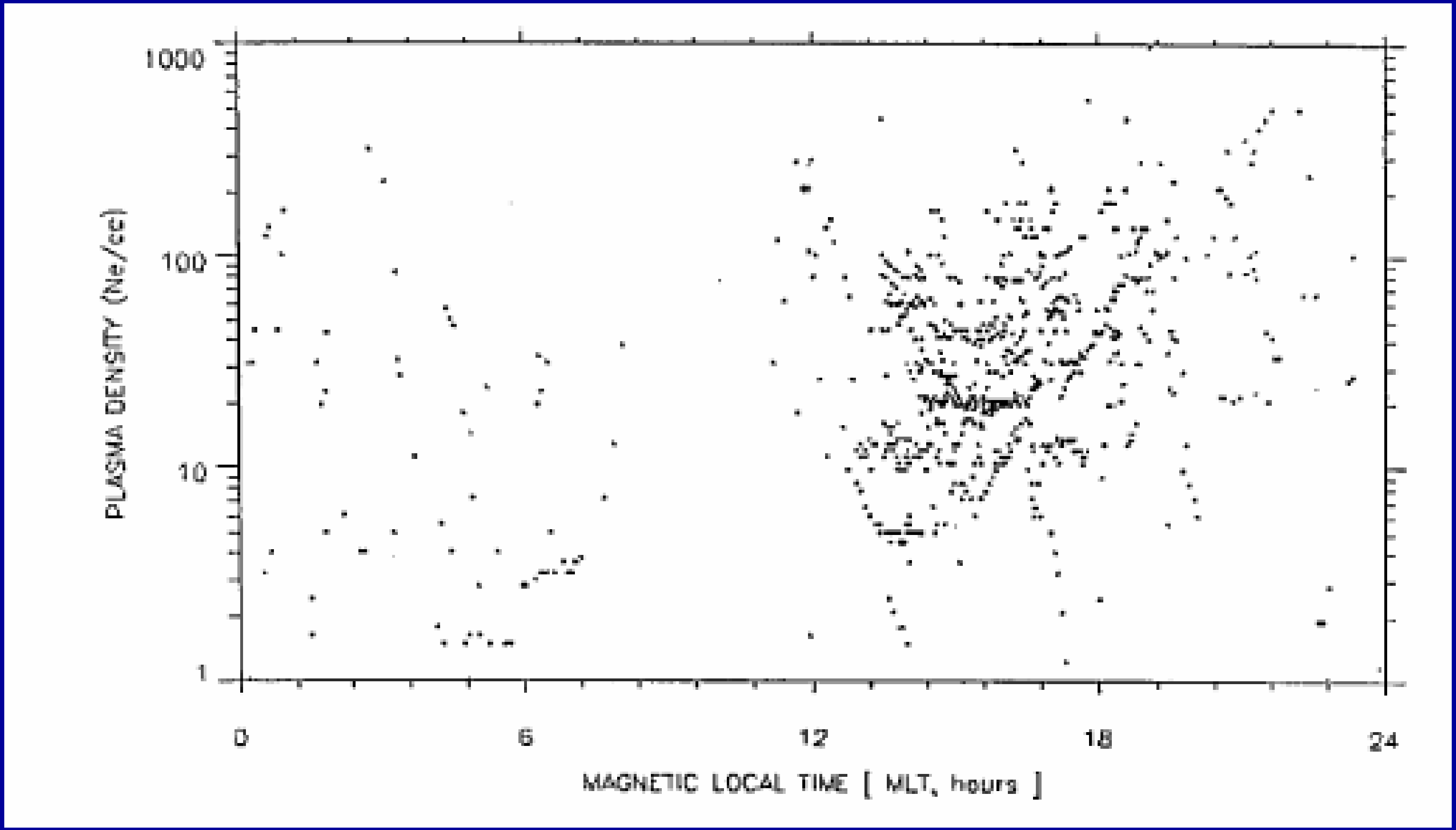

Highest occurrence when thermal density is ~10- 300 cm^{-3} [Fraser and Nguyen, JASTP, 2001]

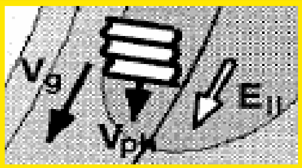

DE-1 Occurrence rates in storm time ~2.3% at L = 3-4; in quiet time ~0.43%

Low occurrence may be due to spatial and temporal variability of waves with only one spacecraft sampling them

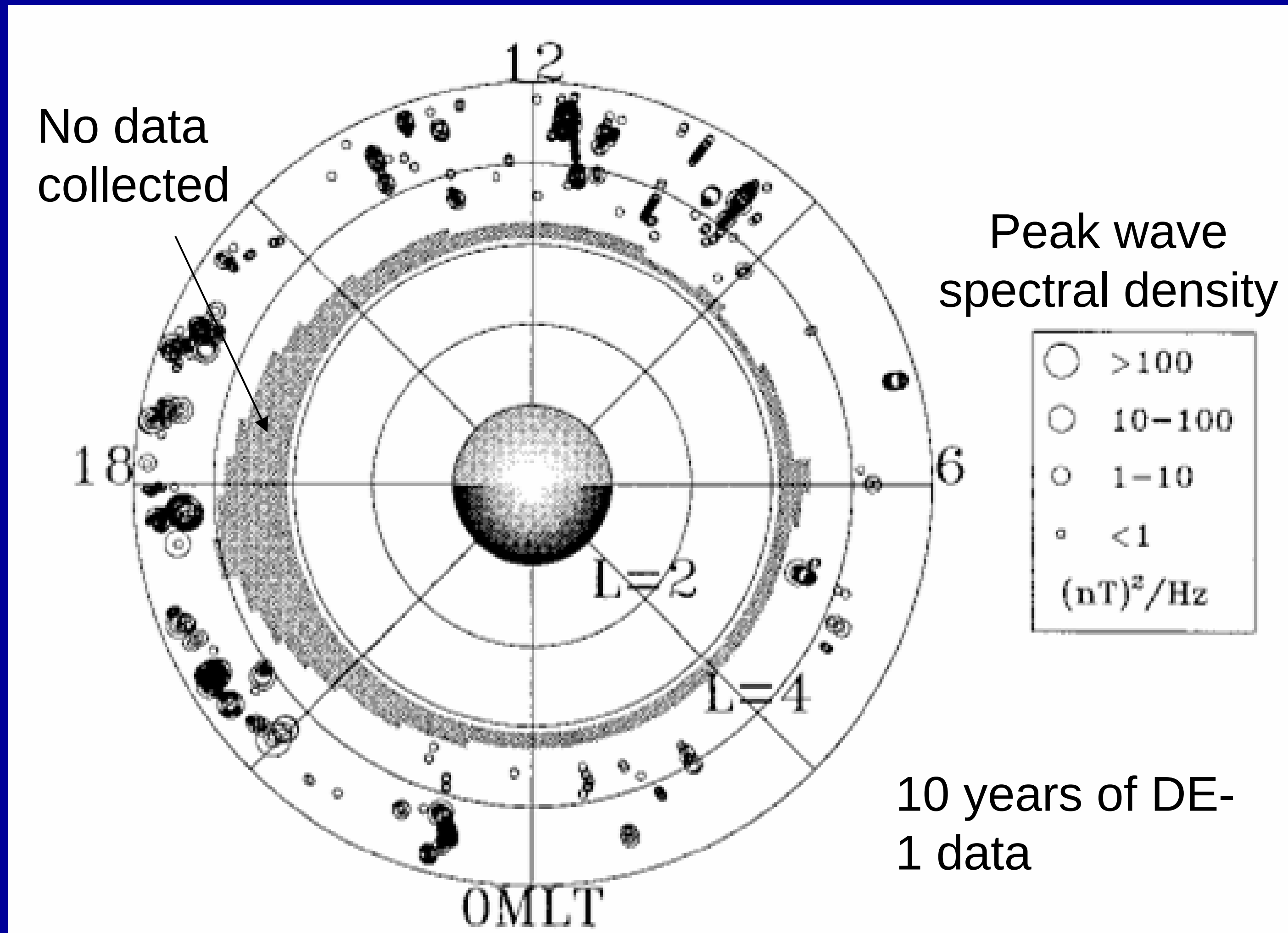

Erlandson & Ukhorskiy, JGR, 2001

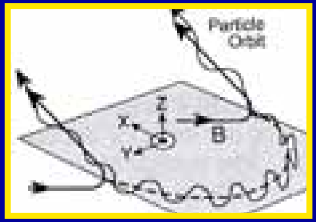

Ion scattering in stretched magnetic fields creates large-scale ion precipitation zones

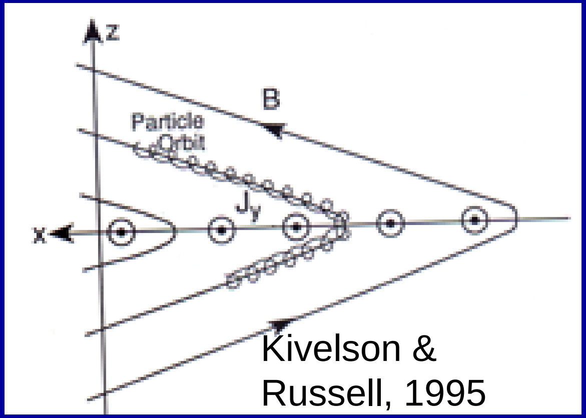

When the ion gyroradius > field line curvature, the particle scatters in pitch angle crossing the equatorial plane. Isotropizes distribution [Sergeev et al., Planet. Space Sci., 1983; Anderson et al., JGR, 1997]

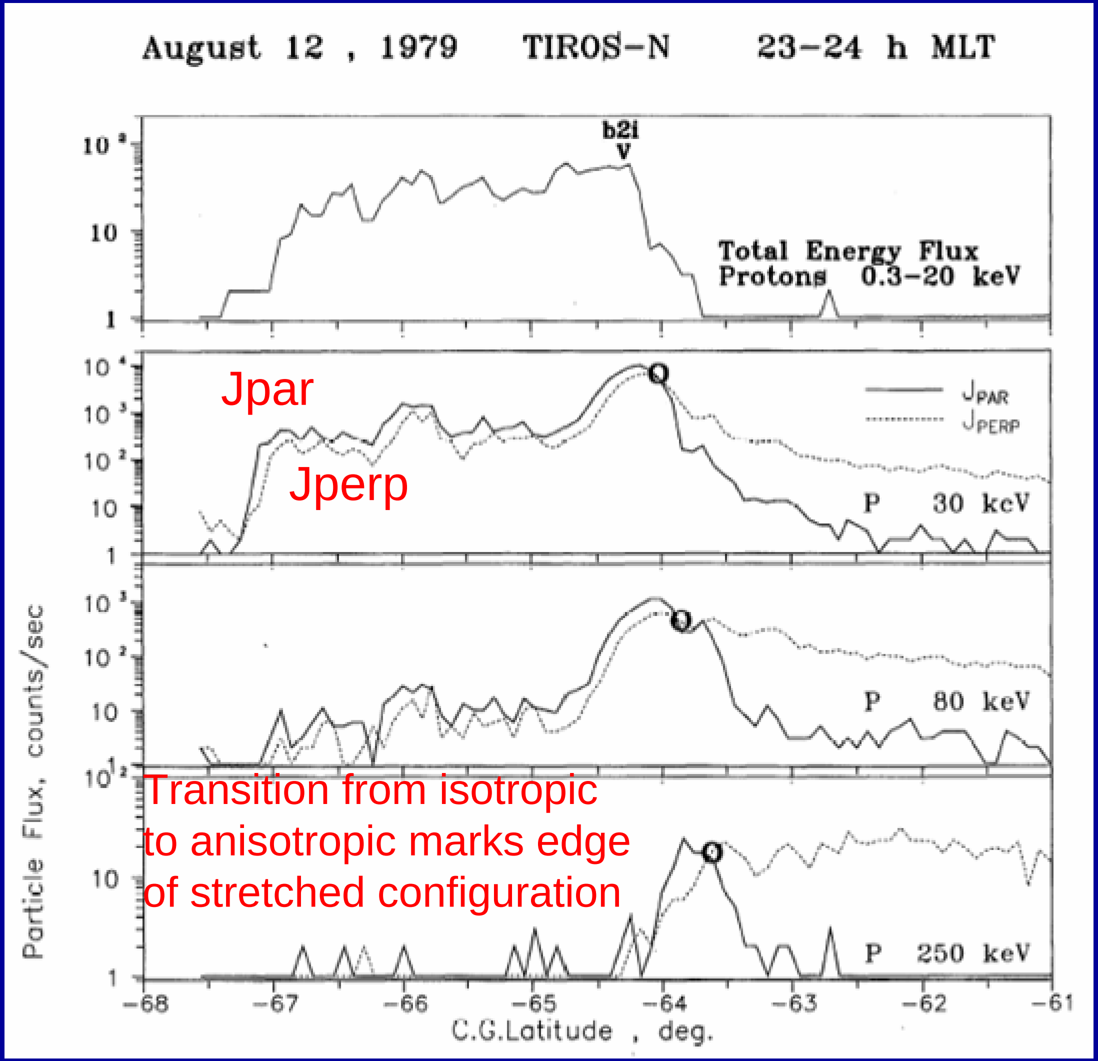

Newell et al., JGR, 1998

Ion scattering in stretched magnetic fields creates large-scale ion precipitation zones

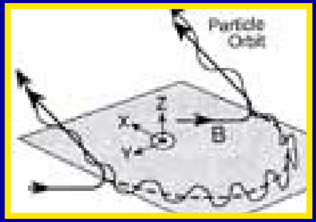

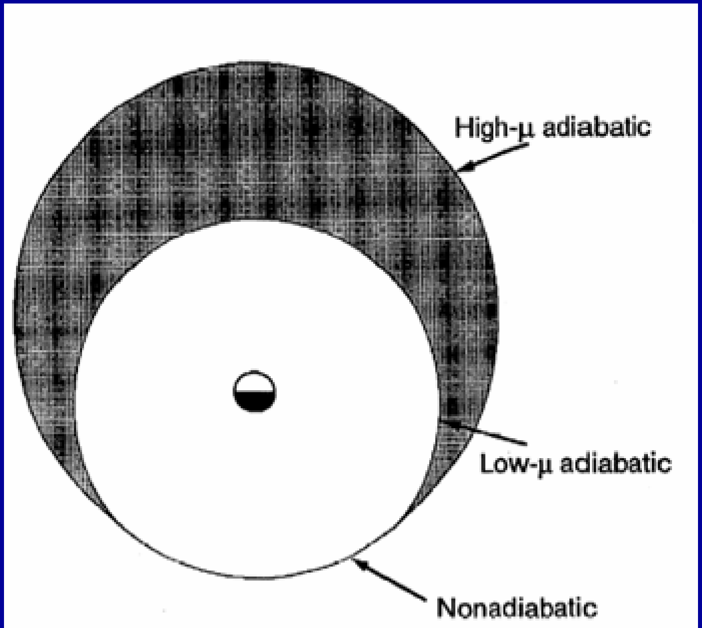

Anderson et al., JGR, 1997

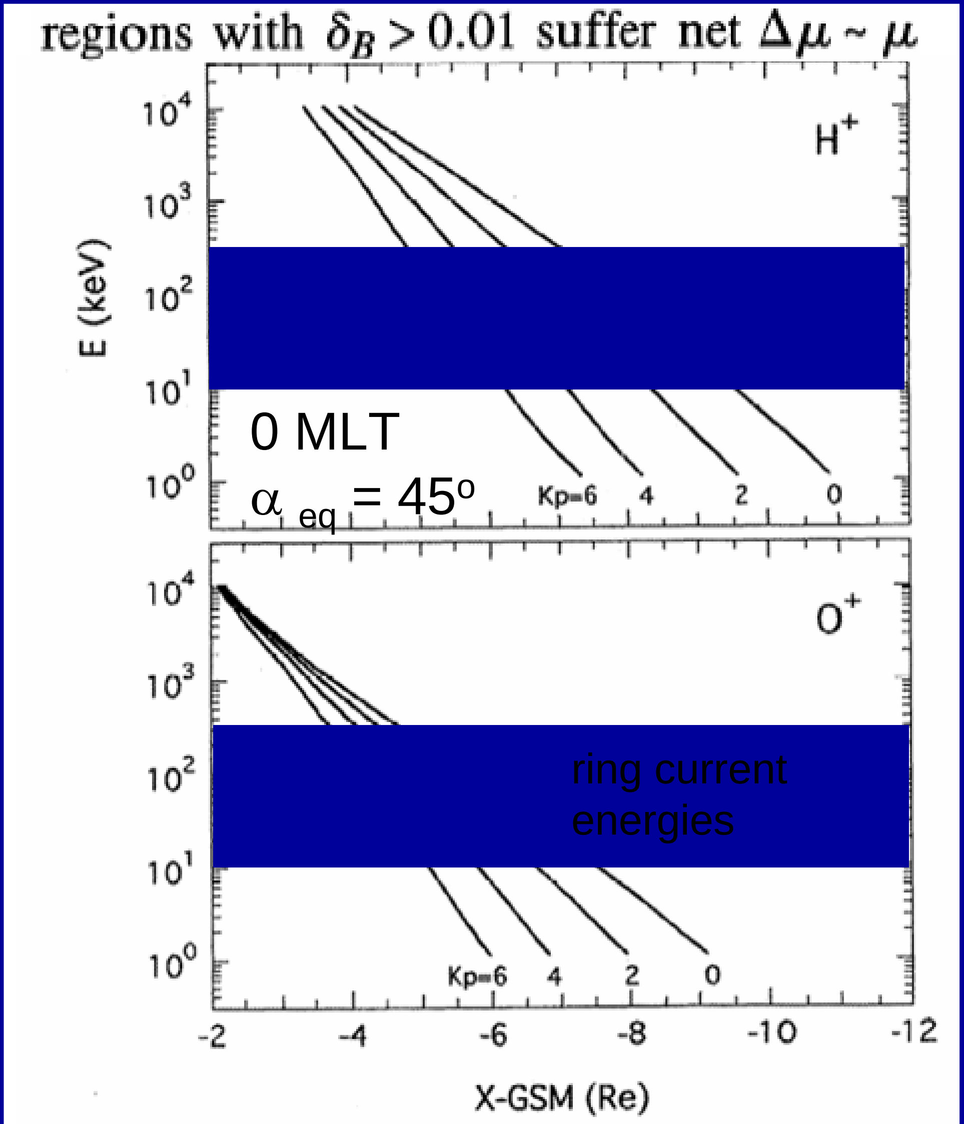

Basics of Charge Exchange

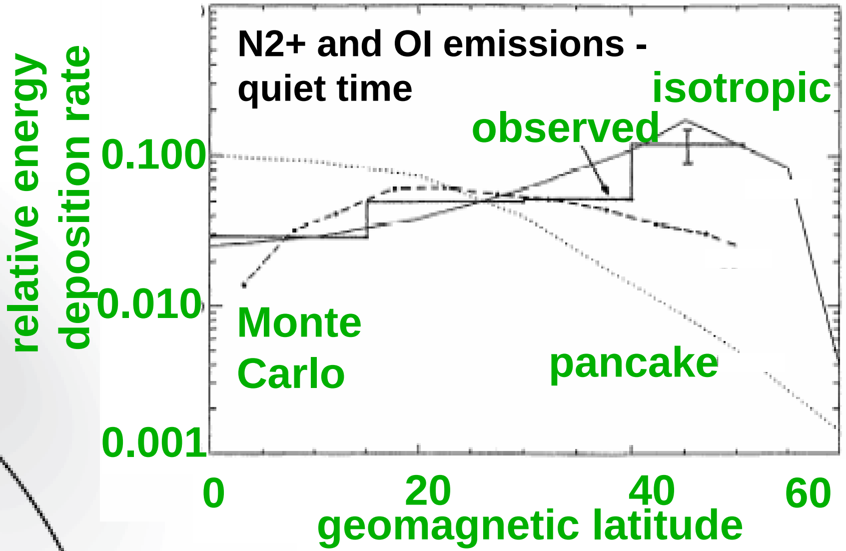

[after Tinsley et al., JGR, 1994]

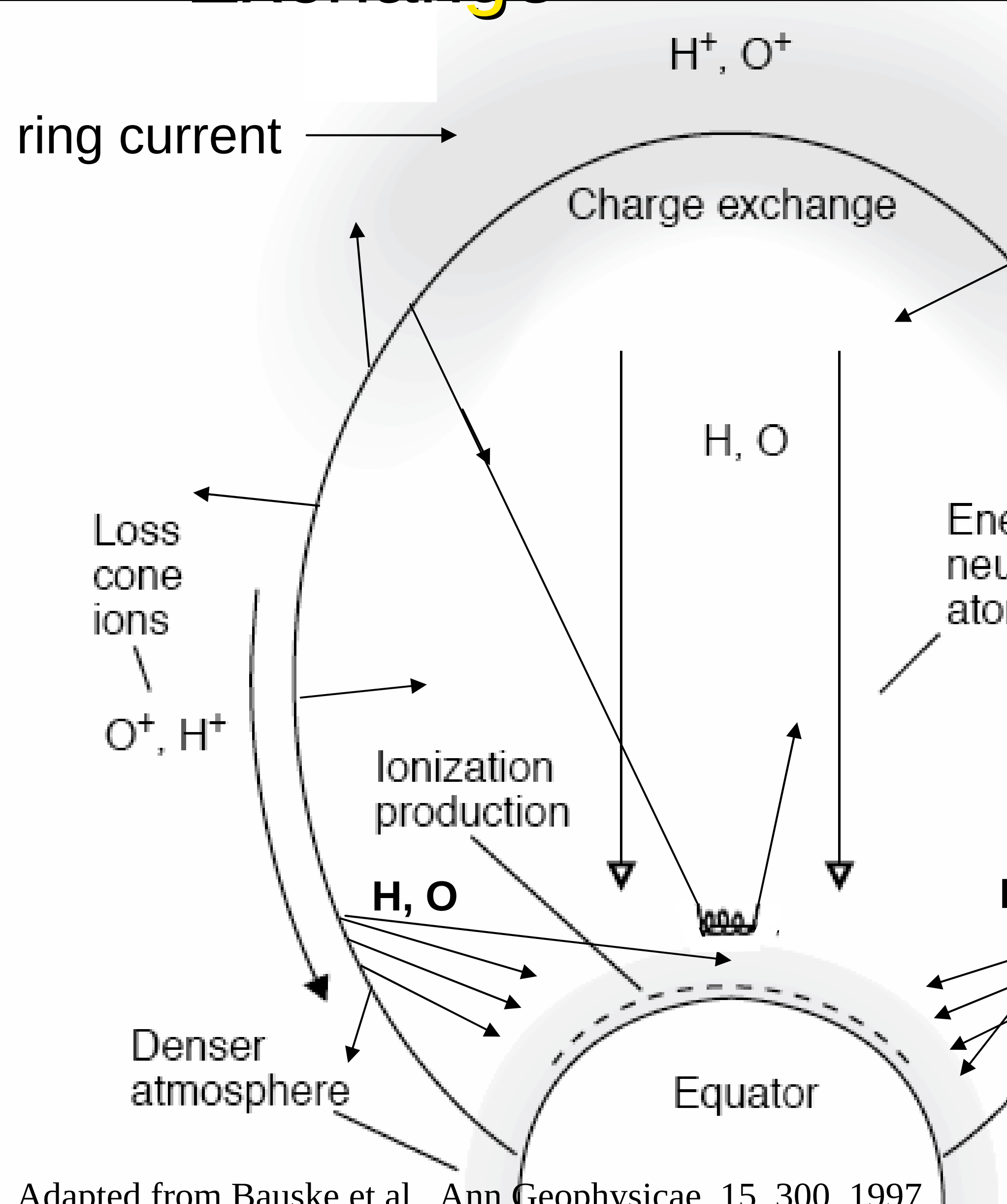

Adapted from Bauske et al., Ann Geophysicae, 15, 300, 1997.

Isotropic ring current: ions mirroring low on field line create most ENA. Peaks in ENA at foot of field line

Pancake ring current: most ions in equatorial plane; peak in ENA at equator

Loss cone ions: form ion/neutral beam at foot of field line.

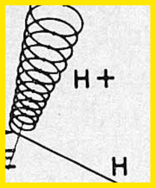

Charge exchange lifetimes vary with species

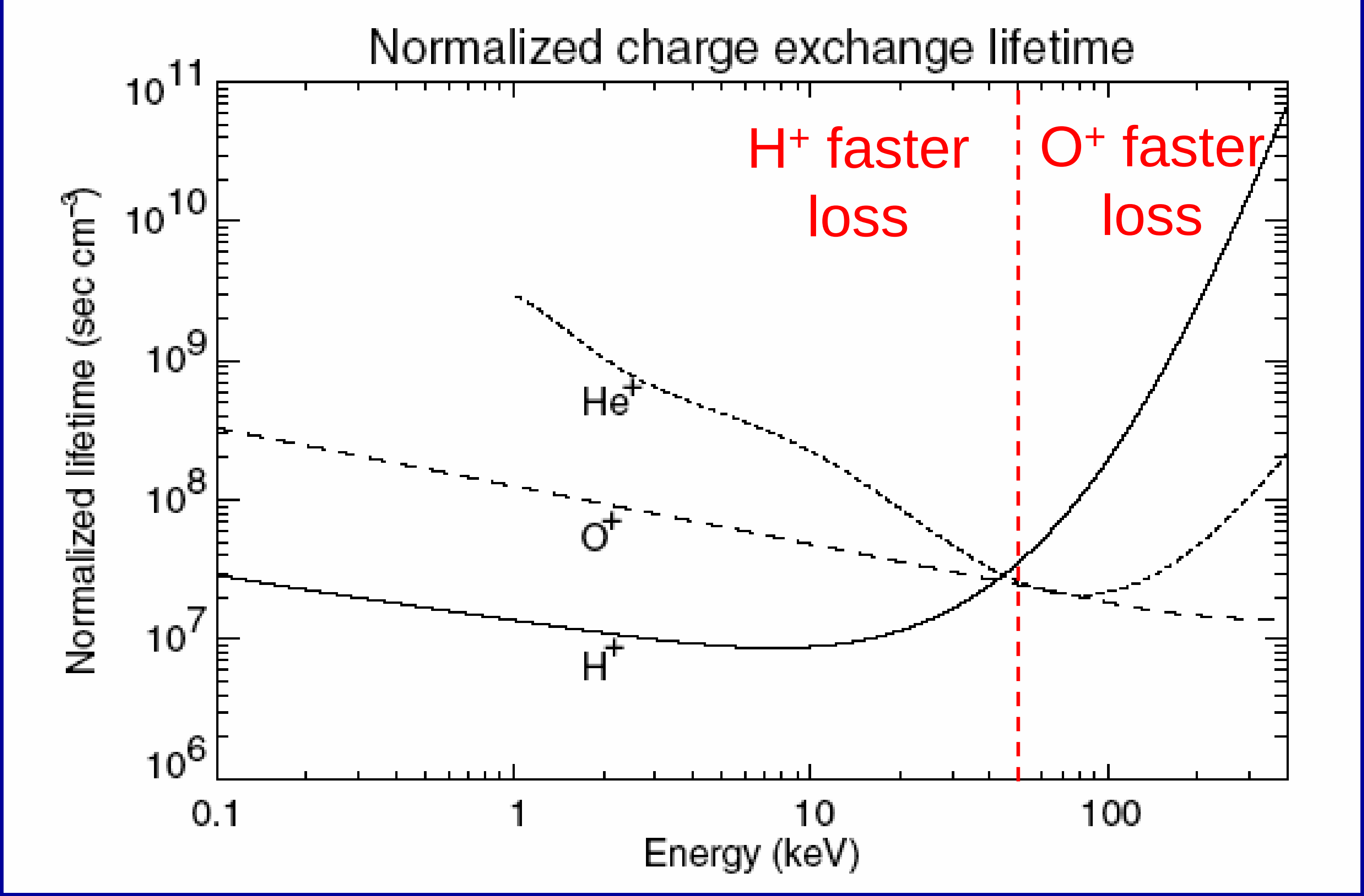

Ebihara and Ejiri, Space Sci Rev, 105, 377-452, 2002.

Relative Importance to Ring Current Energetics

TABLE IV

Loss rates of the total energy content to that calculated with no loss process for different loss processes for different ionic species at an elapsed time of 48 h from the beginning of the calculation. The loss rate of 100% corresponds to that the total energy content is wholly lost

Loss process	H^+ (%)	He^+ (%)	O^+ (%)
No loss	0.0	0.0	0.0%
Charge exchange	65	38	51
Coulomb drag	6.4	9.0	6.8
Drift loss cone	1.6	1.6	1.6
Strong diffusion	82	77	69

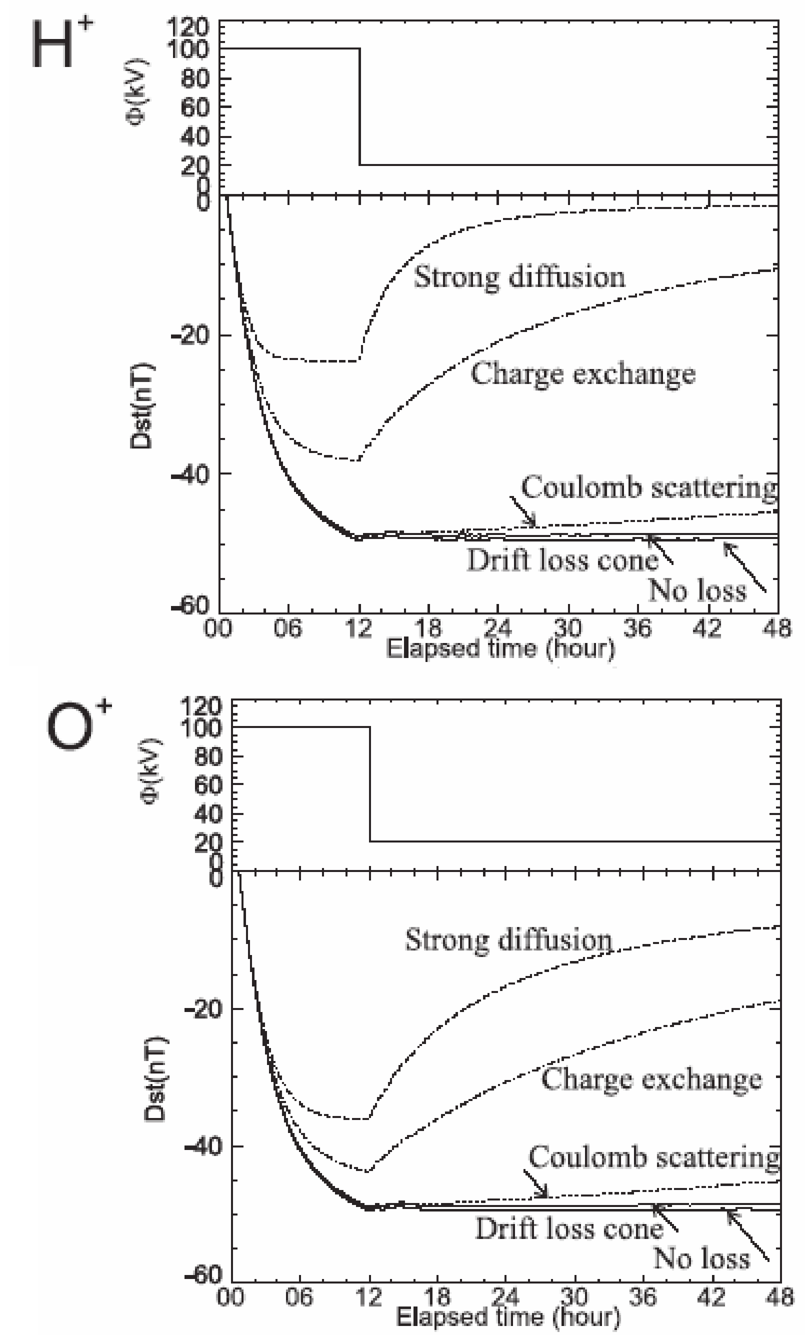

Ebihara and Ejiri, Space Sci Rev, 105, 377-452, 2002.

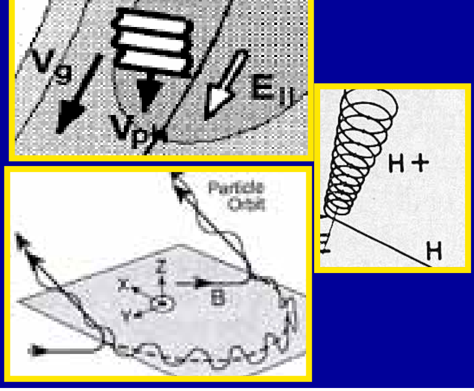

Atmospheric Effects of All Precipitating Particles are Not the Same

Monoenergetic Proton Flux

Unidirectional monoenergetic electron flux

QuickTime™ and a TIFF (LZW) decompressor are needed to see this picture.

QuickTime™ and a TIFF (LZW) decompressor are needed to see this picture.

Rees, Physics & Chemistry of the Upper Atmosphere, Cambridge Univ. Press, 1989

Electrons penetrate deeper than protons of the same energy.

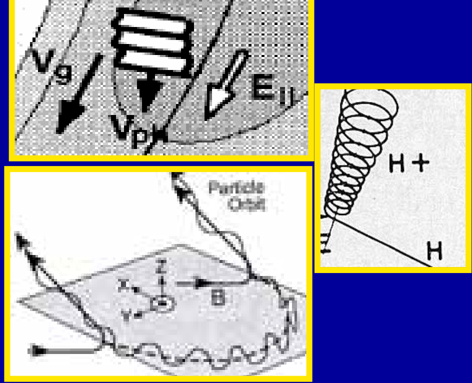

Peak ionization from protons occurs deeper in atmosphere than oxygen of the same energy

Monoenergetic Incident Protons

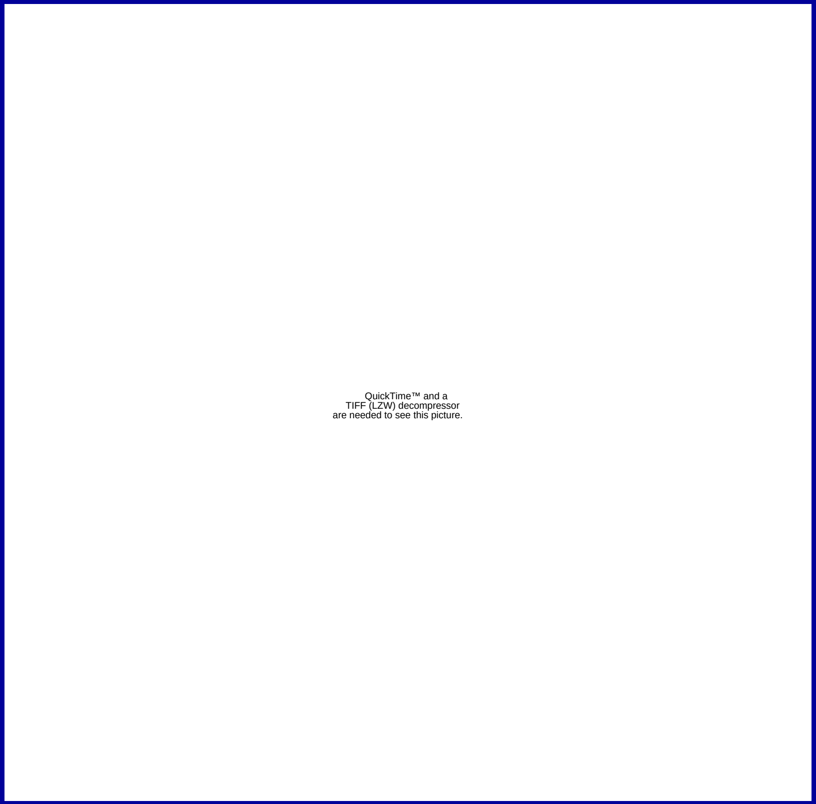

Rees, Physics & Chemistry of the Upper Atmosphere, Cambridge Univ. Press, 1989

Peak Altitude of Ionization as a Function of Incident O^+ Energy

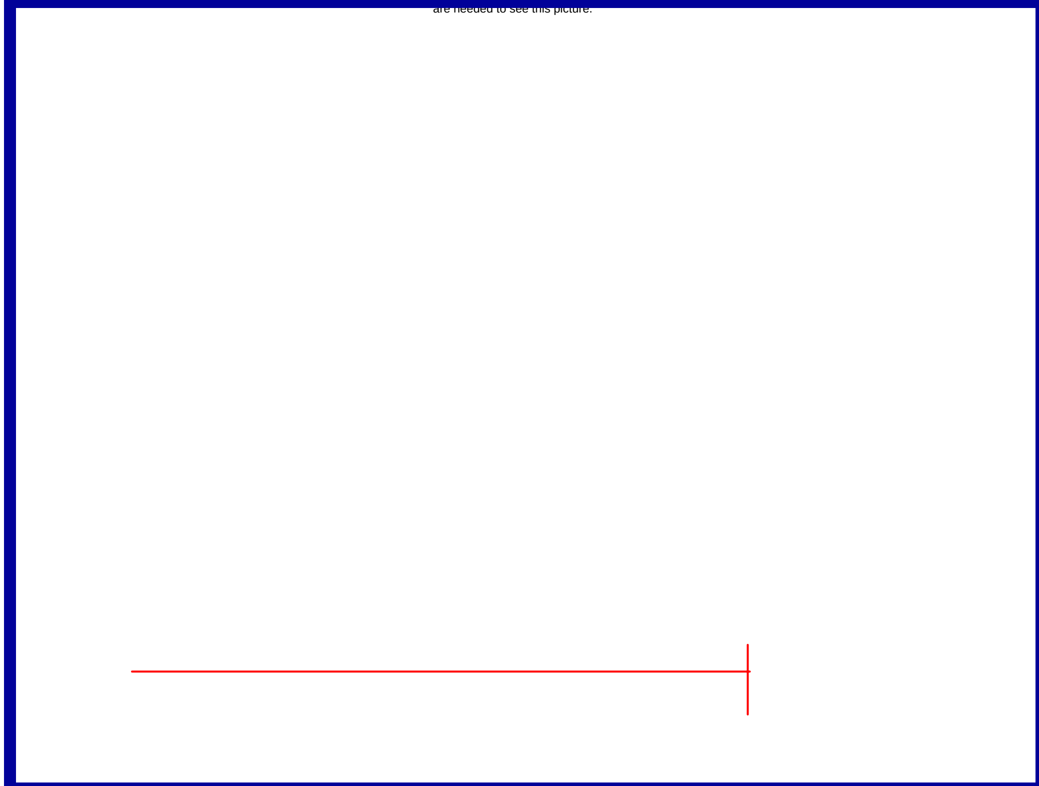

Ishimoto et al., JGR, 8619, 1992

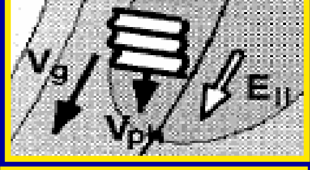

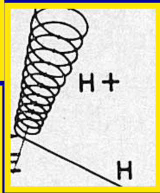

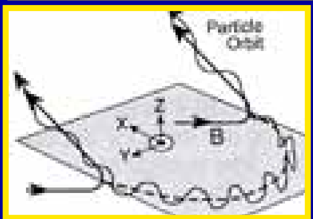

All Ion or Neutral Atom Precipitation Quickly Creates Ion/Neutral Equilibrium Beam

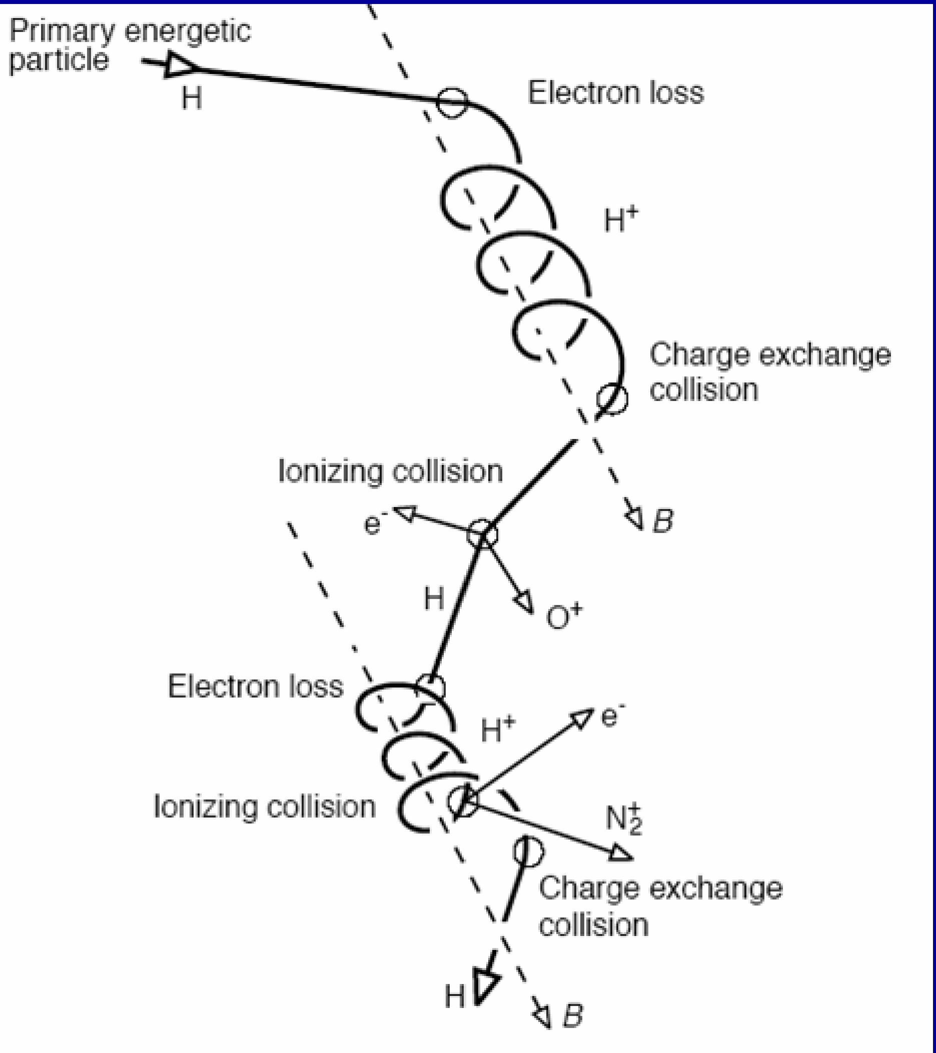

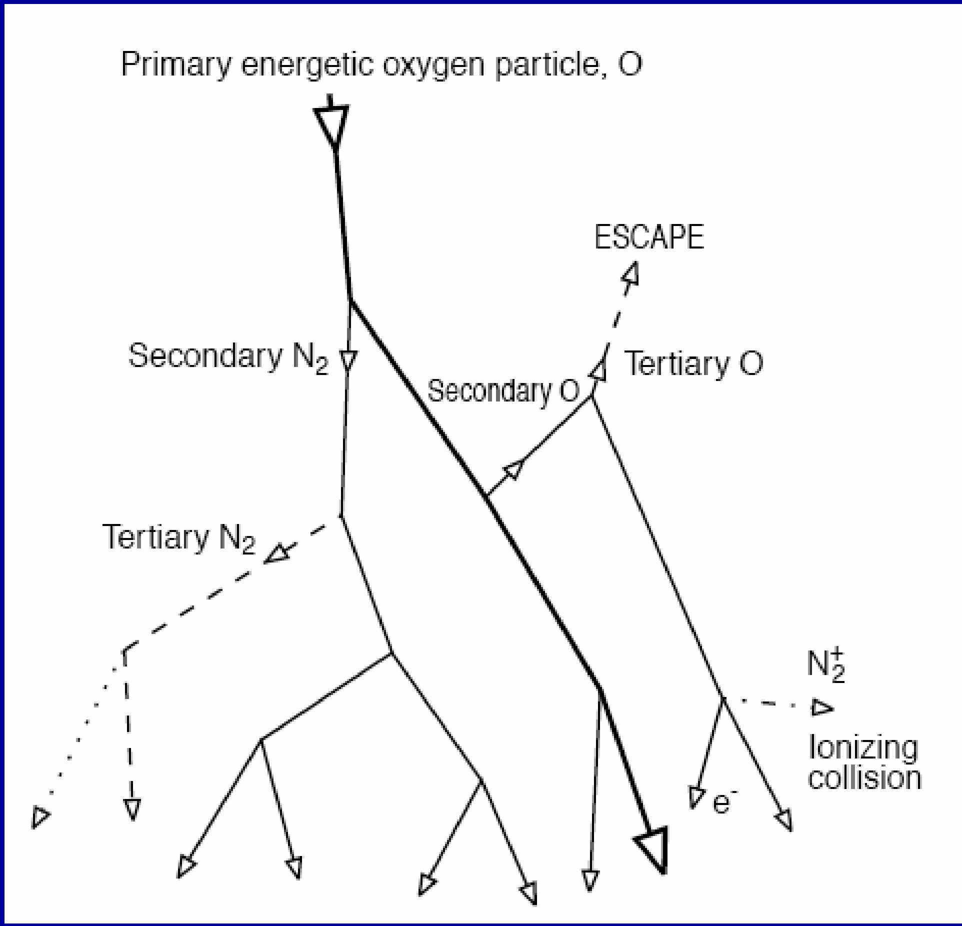

from Bauske et al., Ann Geophysicae, 15, 300, 1997.

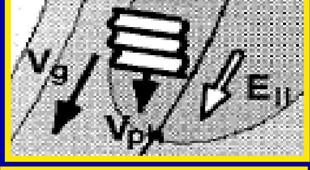

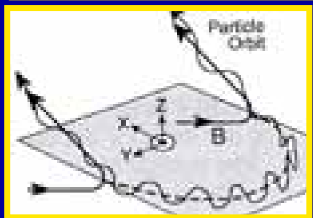

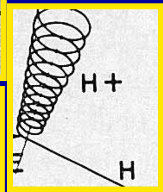

Backsplash Flux of Ions/Neutrals is Produced

Trajectories of 1000 2-keV protons in Monte Carlo model.

Trajectories with upward velocity component produce escape flux which is up to 16% of incident <10 keV flux and 10% for a incident 100 keV flux for 30 deg field tilt

[Synnes et al., JASTP, 1998]

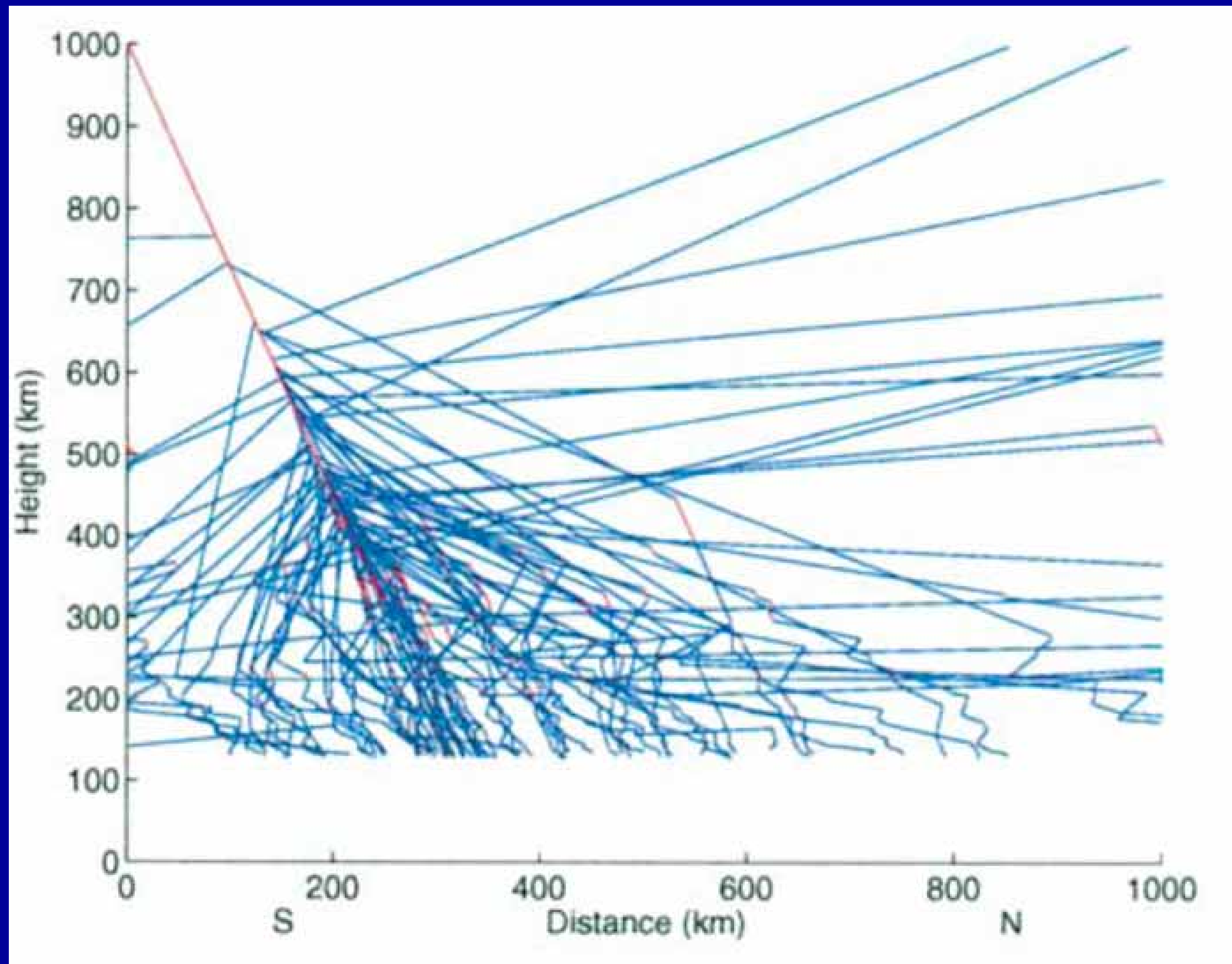

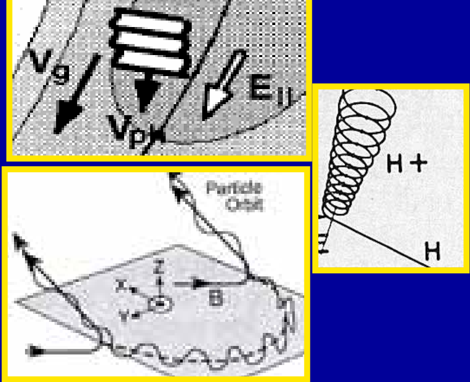

H backsplash is negligible compared to O Backsplash

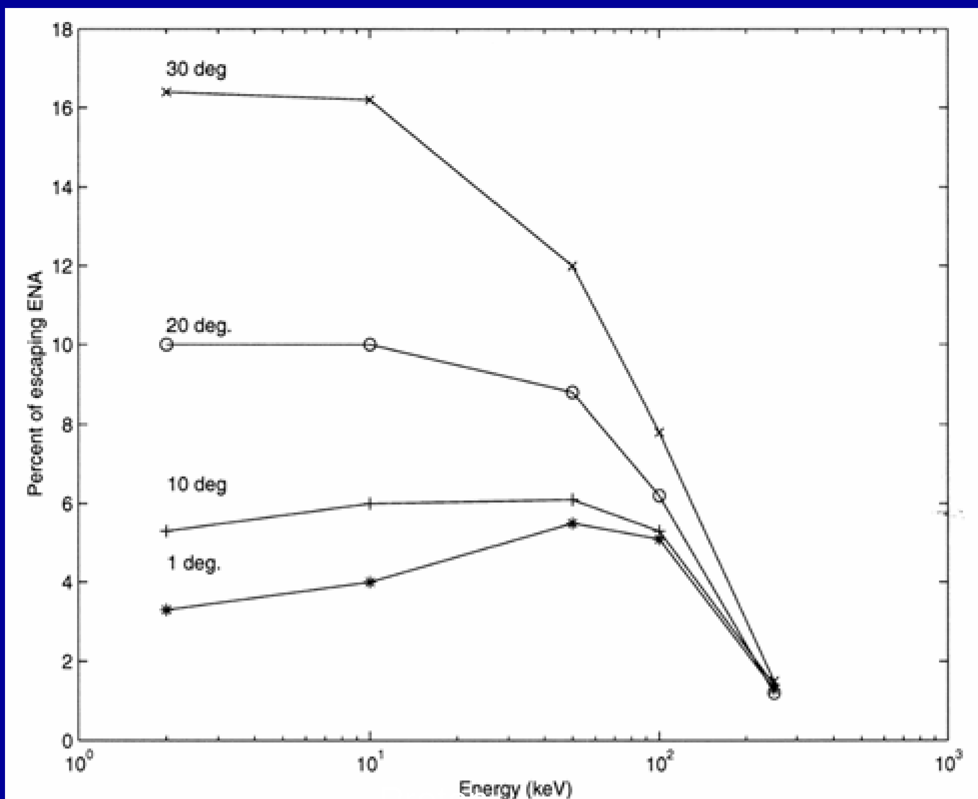

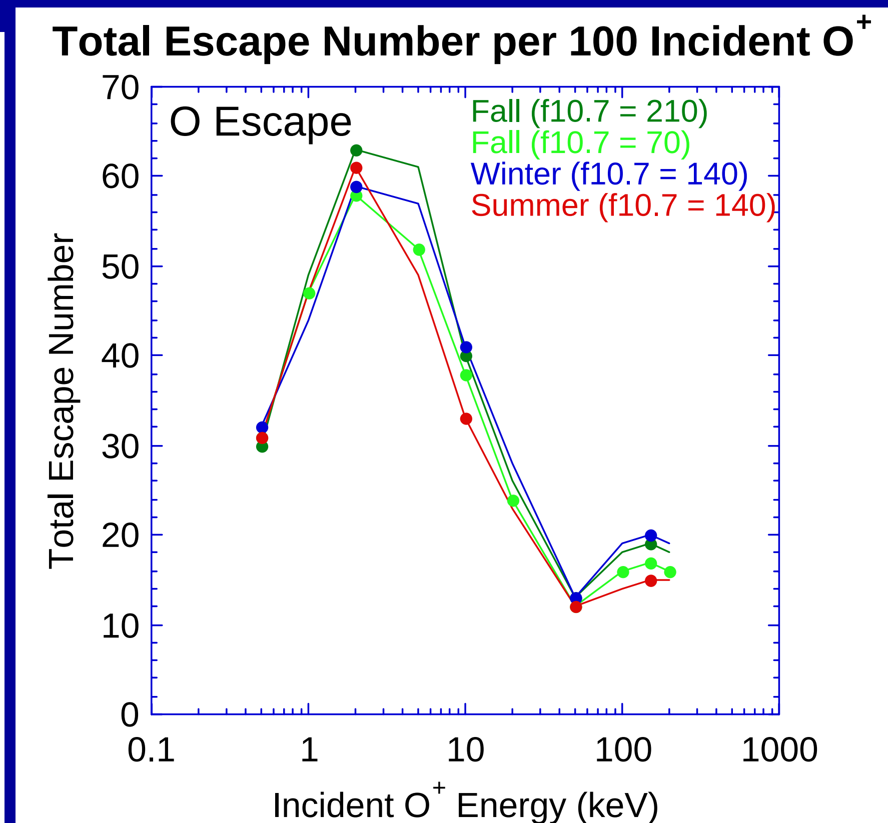

Synnes et al., JASTP, 60, 1695-1705, 1998

Ishimoto et al., JGR, 8619, 1992

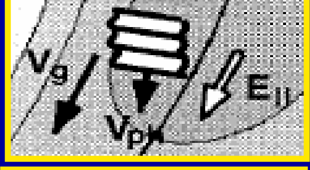

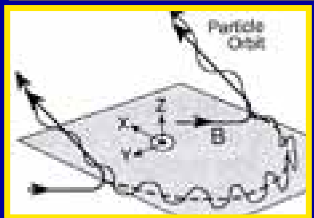

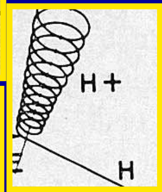

Main dispersion of proton beam takes place between 250 and 450 km. Below 120 km, beam is attenuated dramatically

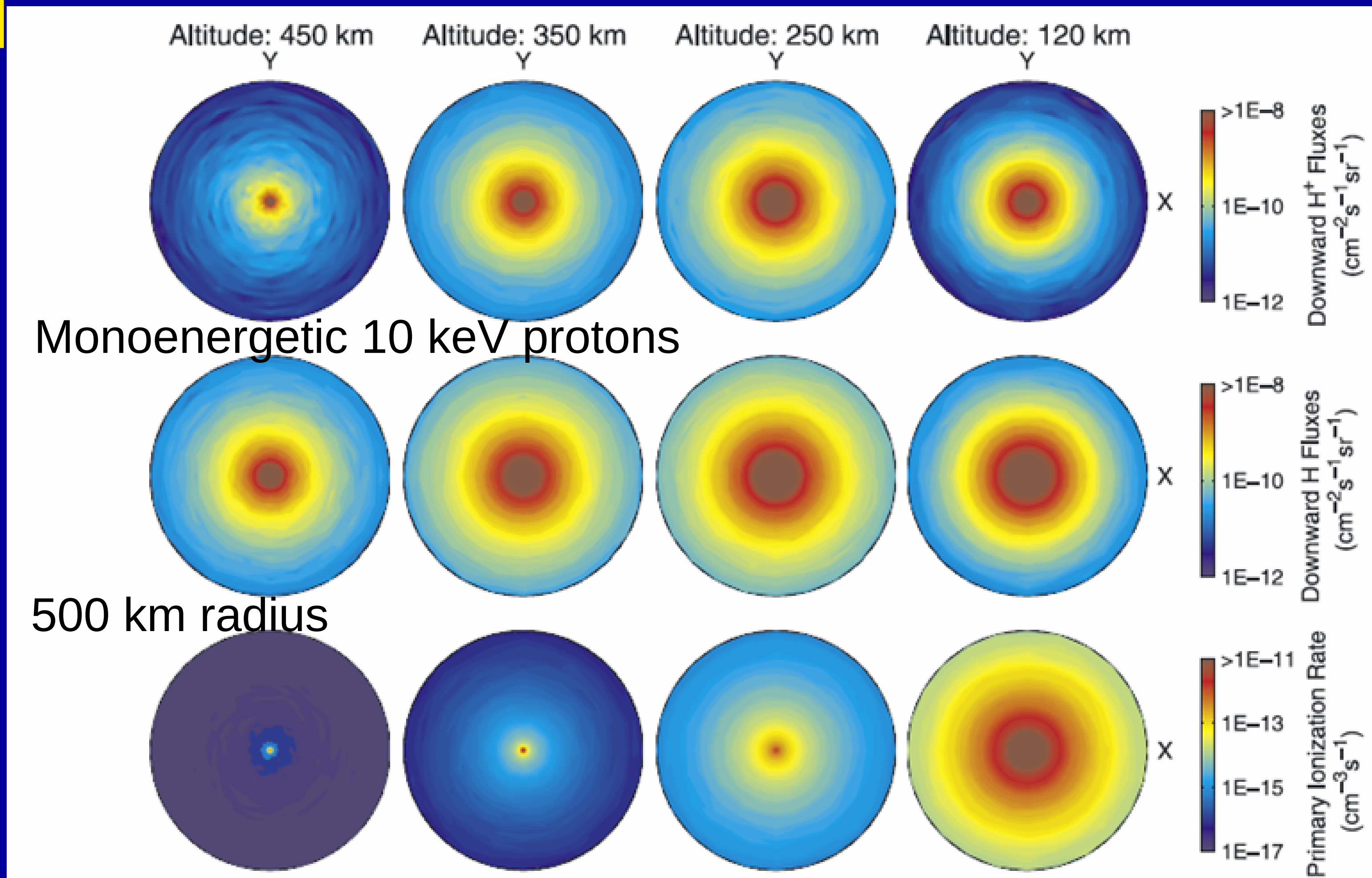

Fang et al., JGR, 2004

Large part of precipitating O^+/O energy heats the neutral atmosphere

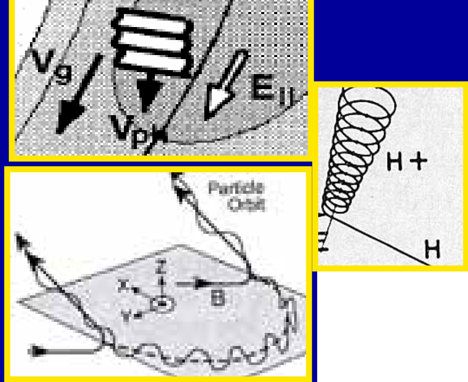

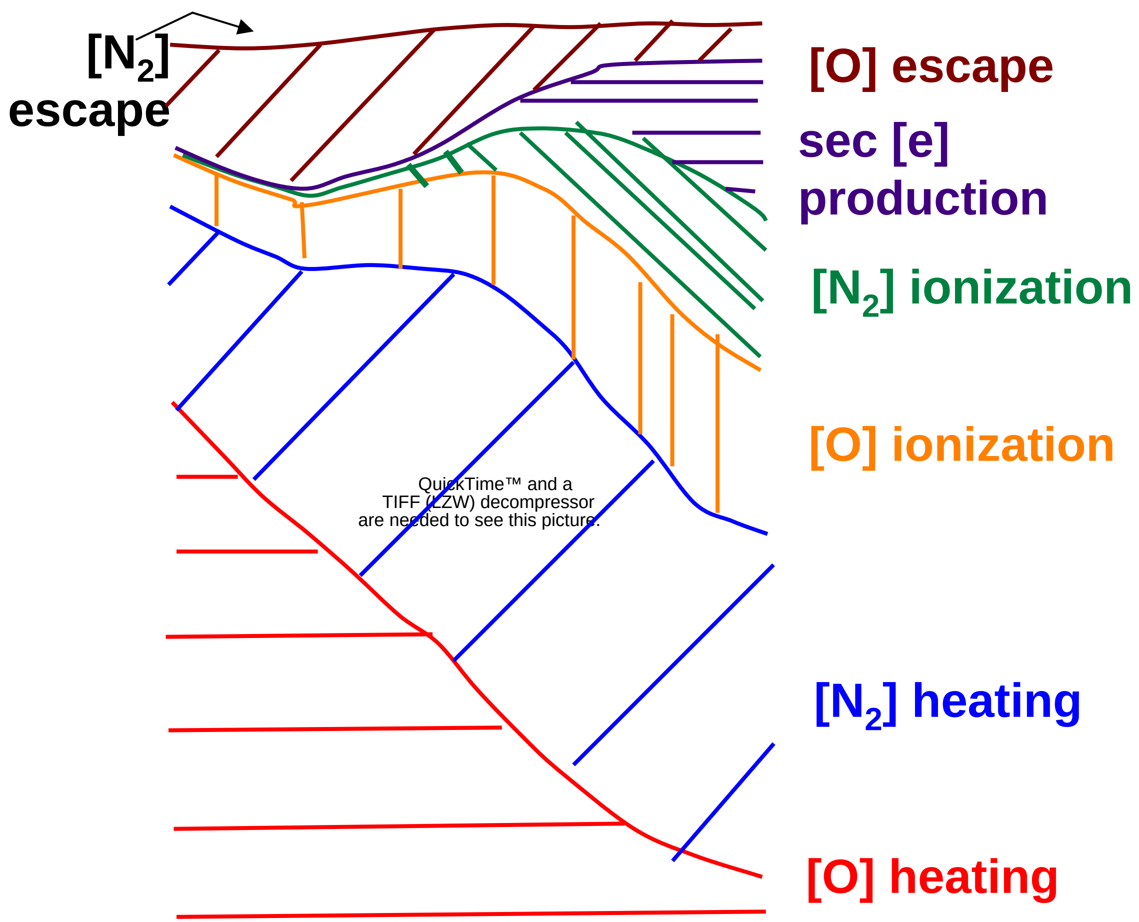

Ishimoto et al.,
JGR, 8619, 1992

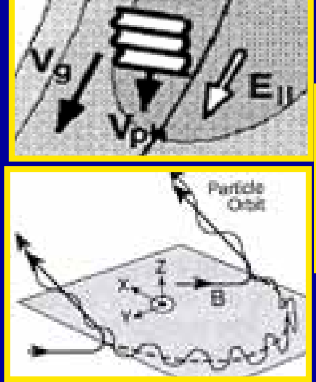

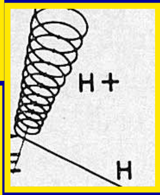

Largest part of precipitating H^+/H energy ionizes & creates secondary electrons

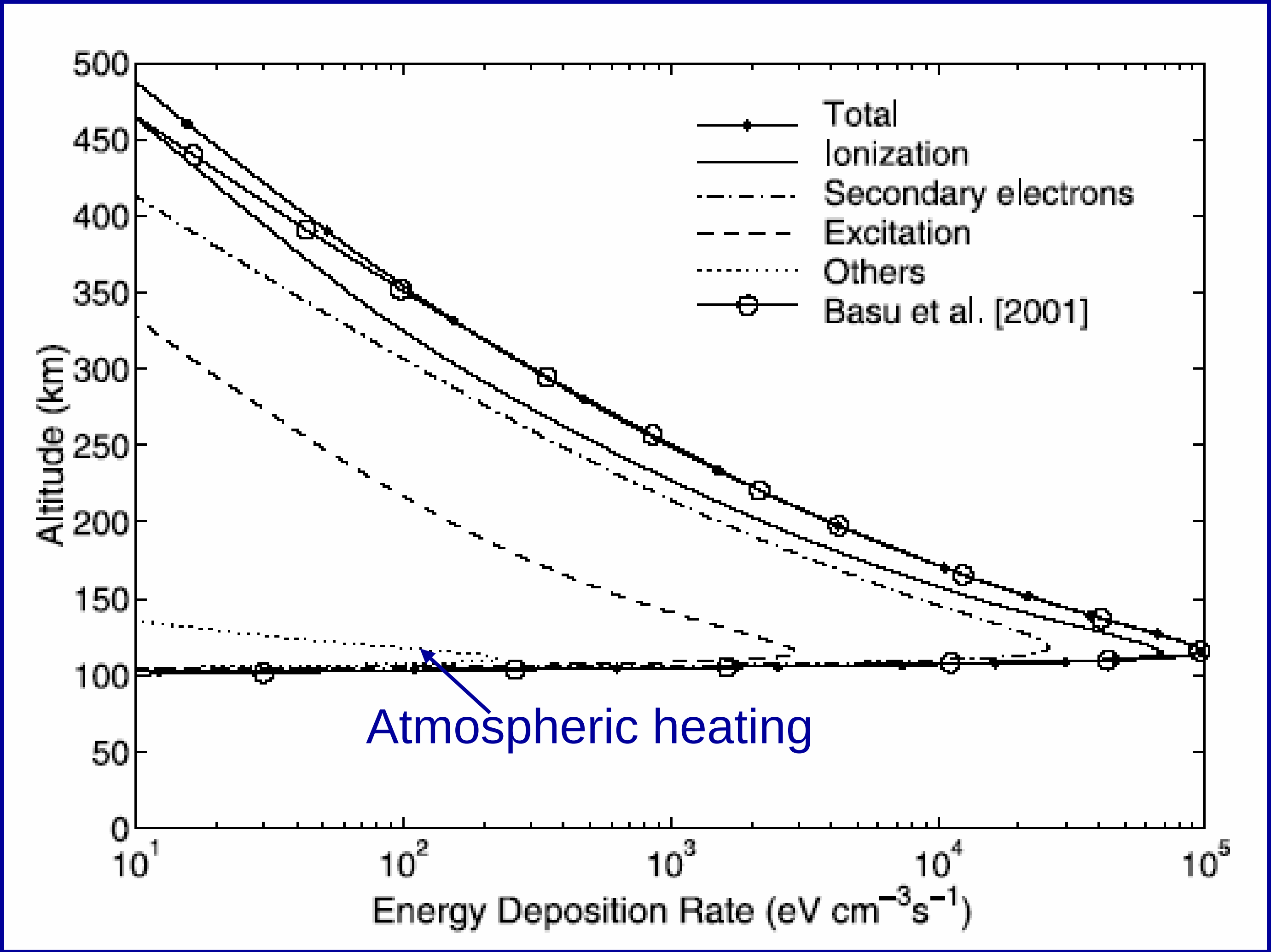

Fang et al., JGR, 2004

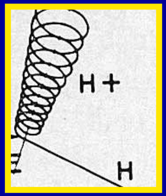

ENA/atom precipitation creates enhanced ionization & conductance, at subauroral latitudes

Simulation of 20-21 April 1985 magnetic storm using AMPTE observations [Bauske et al., 1997]

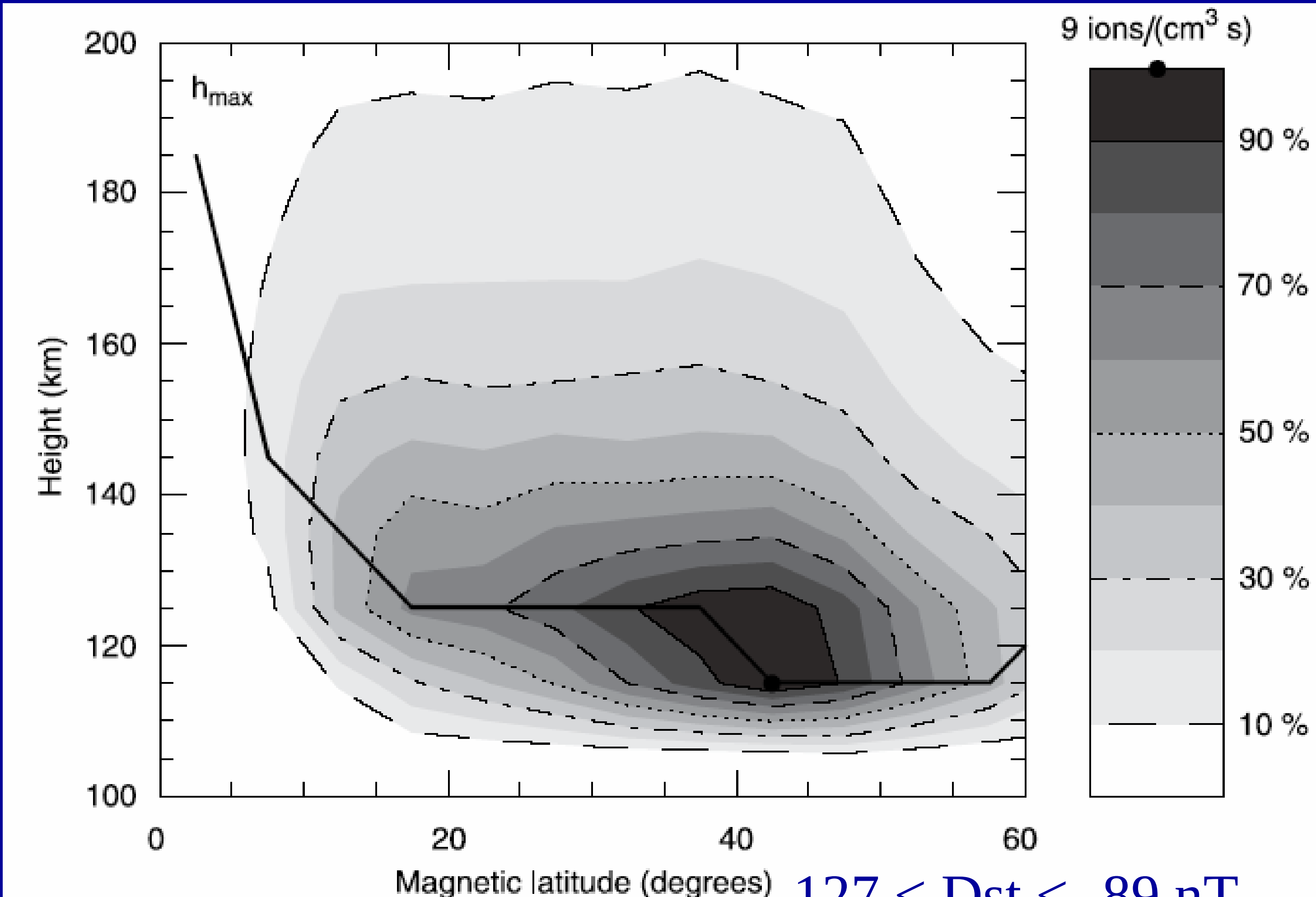

-127 < Dst < -89 nT

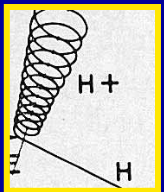

Factor of 5-10 Enhancement in Ne for a Major Magnetic Storm at Low Latitudes

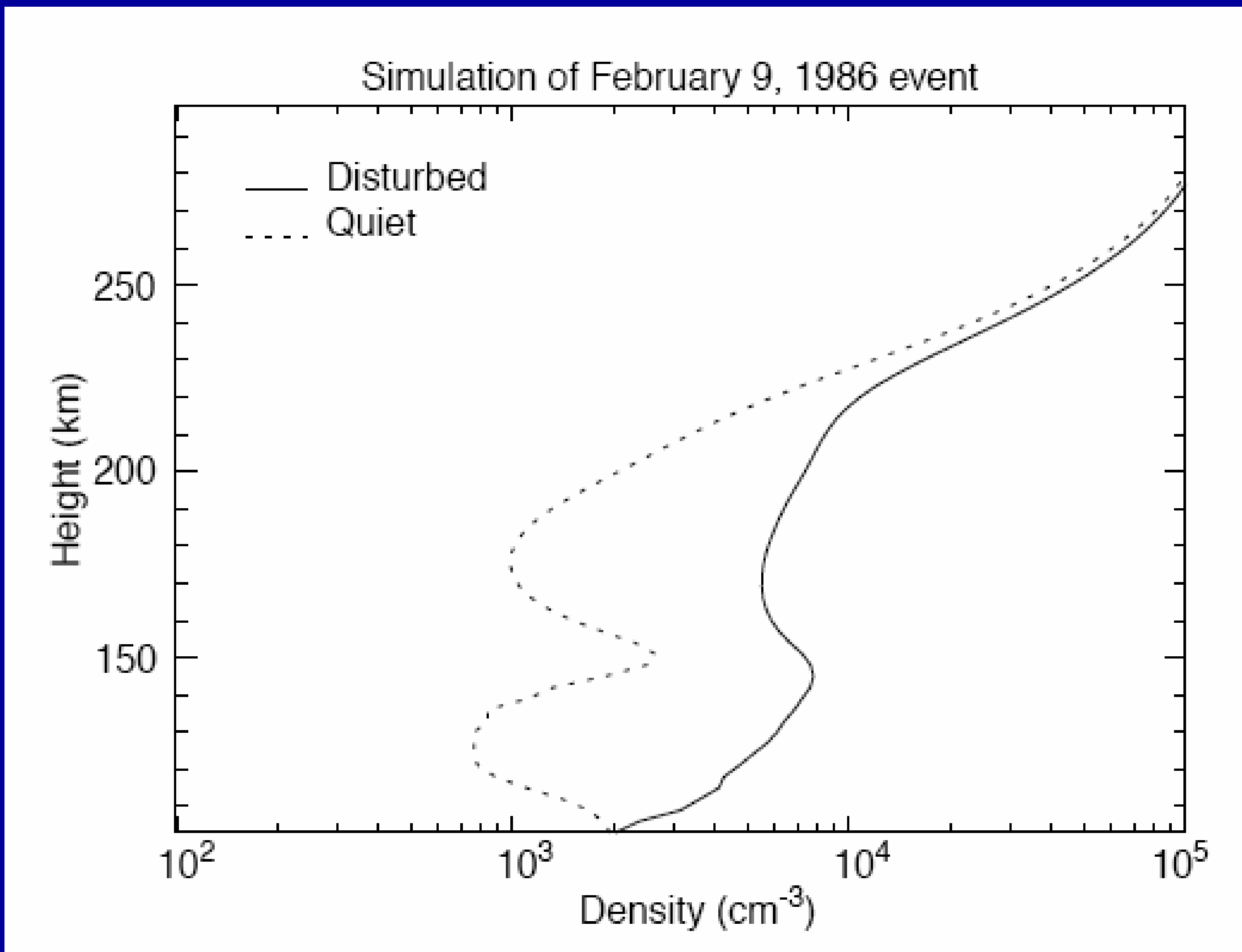

Bauske et al., 1997

Simulation for a location close to Arecibo.

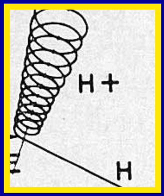

Global View of Ionization Contribution Using 3-hr NOAA Proton Plots

NOAA / POES data

30-240 keV proton energy flux

Model results

Ionization peak intensity

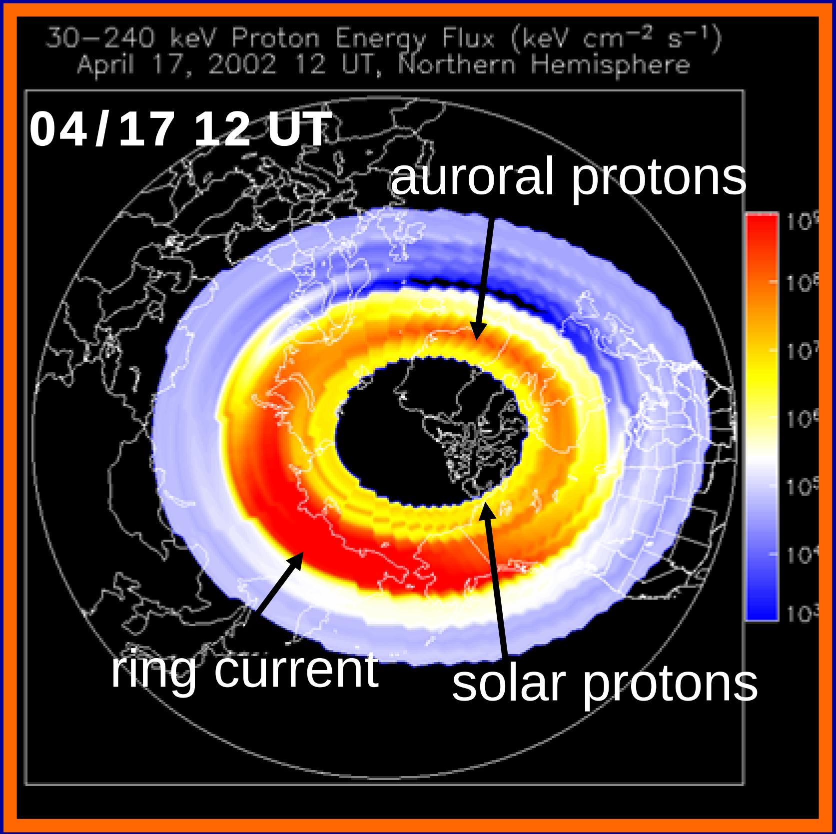

Fang et al., 2004 model

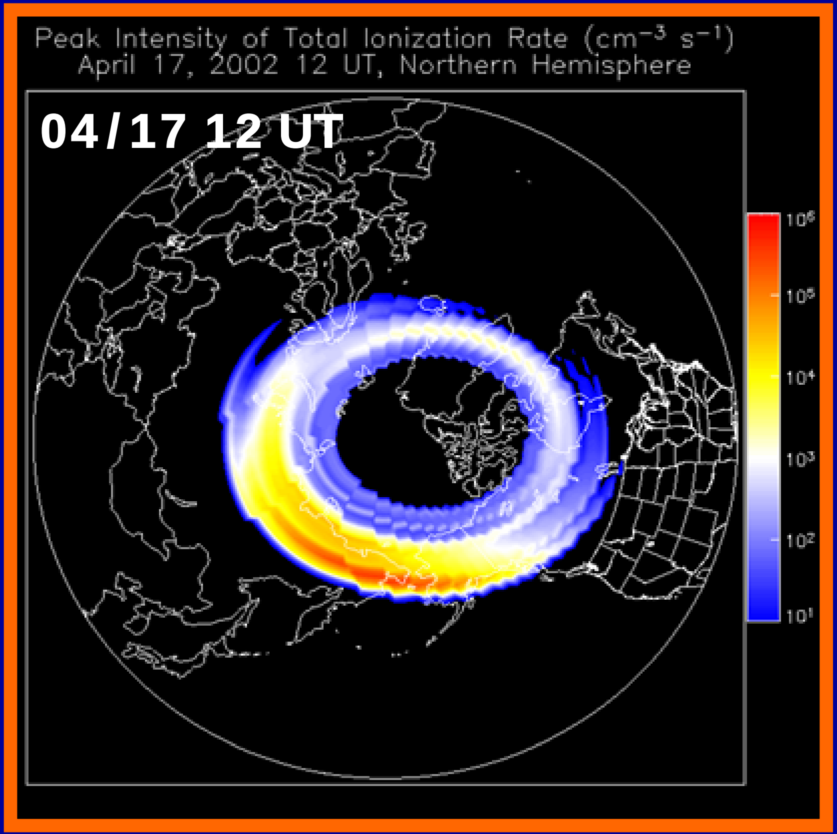

New Information on the subauroral and equatorial effects

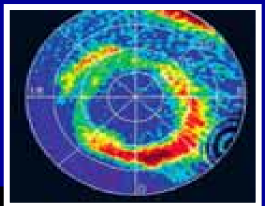

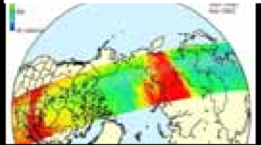

- Midlatitude/Equatorial Ion Auroras
  - Detached Proton Arcs
  - Mid-to-Low latitude ENA/Ion Auroras
- Visible SAR arcs
  - Subauroral Te peaks exceeding 10,000 K
  - Morningside extension
  - Soft ion source population

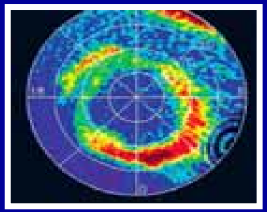

Detached Proton Arcs Indicate Wave-Particle Interactions Are Occurring in Regions that Map Subauroral

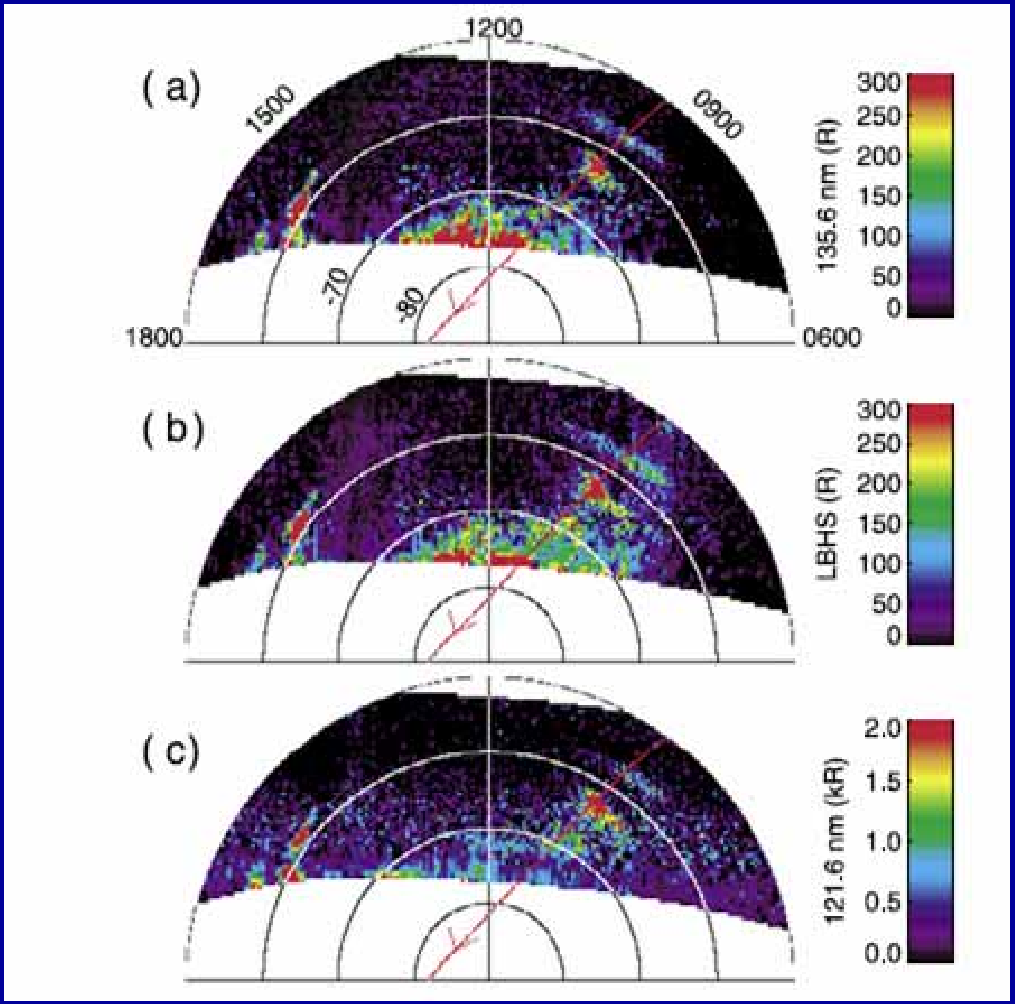

Detached arcs in subauroral region reported Moshupi et al., [2000], Anger et al., [1978]; Vondrak et al., 1983].

Immel et al., [2002]: protons are major source of duskside detached arcs from IMAGE

Zhang et al. [2002]: dayside detached arcs related to NW IMF & pressure hits seen by IMAGE.

Auroral images from TIMED/GUVI show double detached arcs, morning & afternoon, 1738 UT, 19 Aug 2003 [Zhang, et al., GRL, 2004]

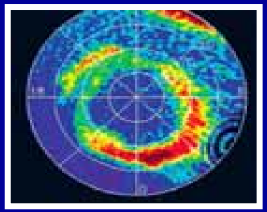

First direct mapping of observed detached arc to drainage plume which is a preferred location for wave activity

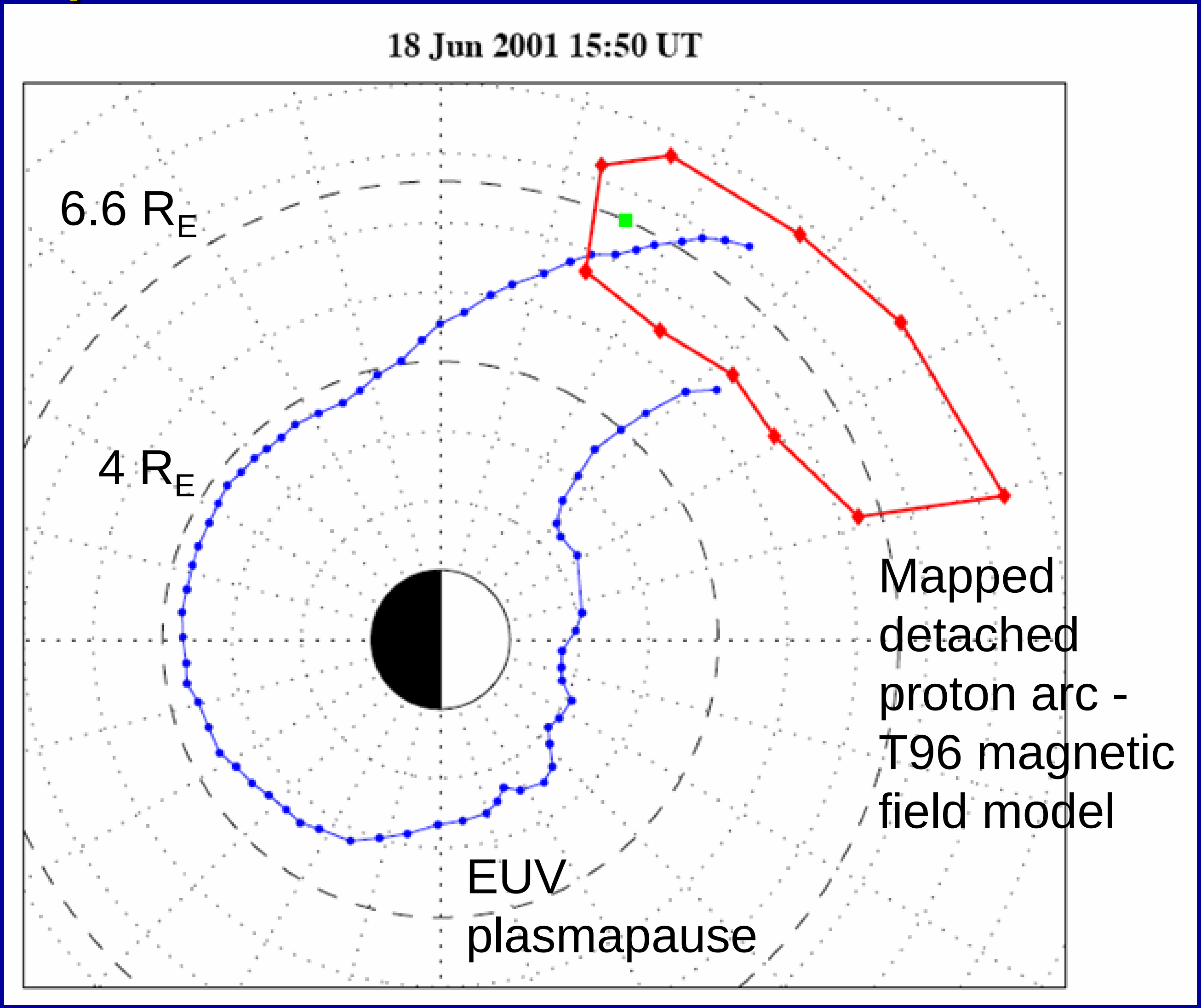

Spasojevic, al., GRL, 2004

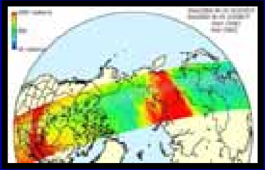

ARGOS observed an O$^+$/O aurora in the SH during the July 2000 Superstorm

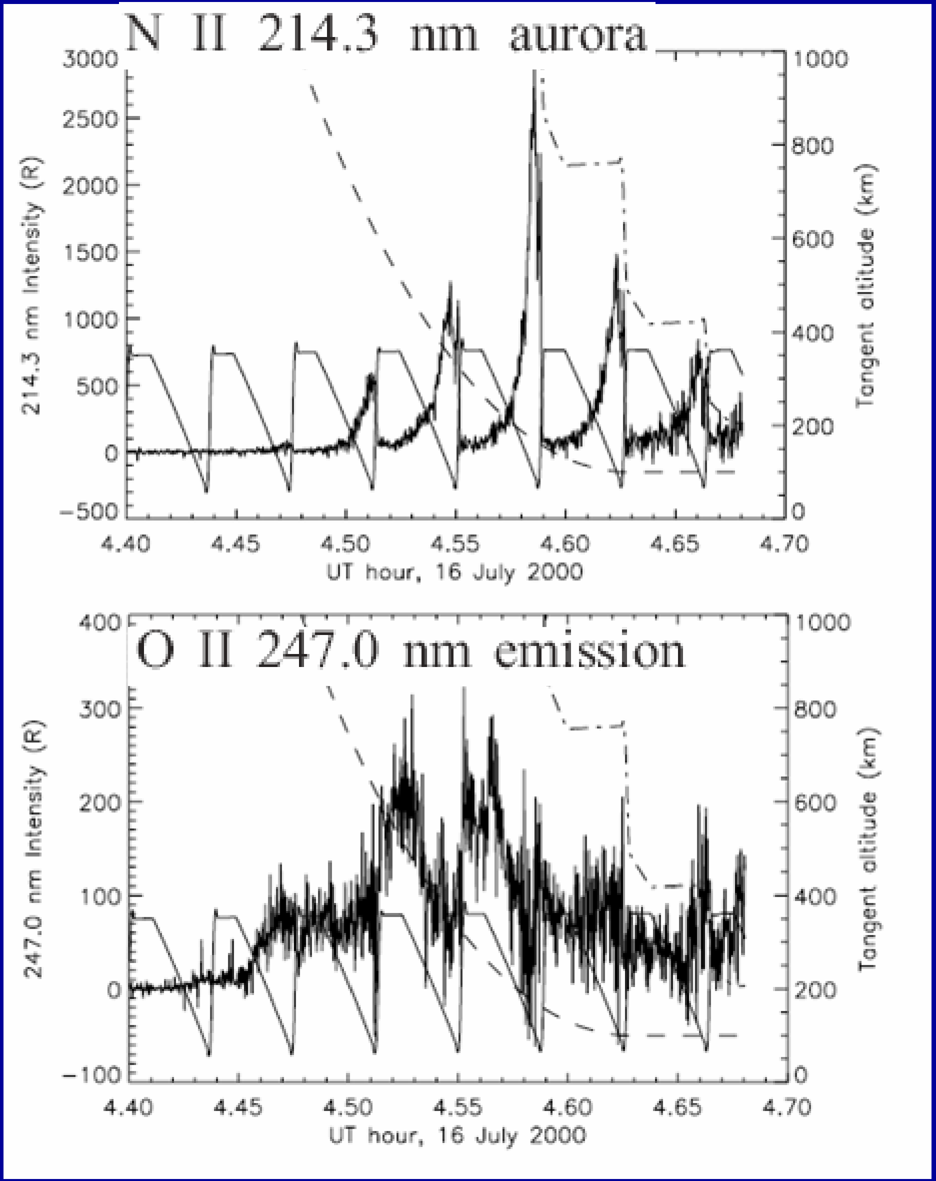

- Enhancement in O and O+ UV emissions during fast recovery of July 2000 major storm.
- Not directly correlated with emissions associated with protons or with electron excitation of N
- Above 300 km, equatorward of the auroral oval, dusk sector, L~4.
- Suggest ring current O ions scatter into loss cone and precipitate. Question: How significant to ring current recovery?

Stephan et al., JGR, 109, A09208, doi:10.1029/2004JA010557, 2004

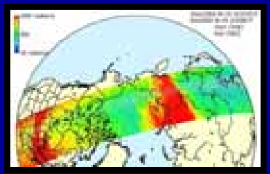

IMAGE/EUV has global view of feature that is consistent with ARGOS observations of an O aurora

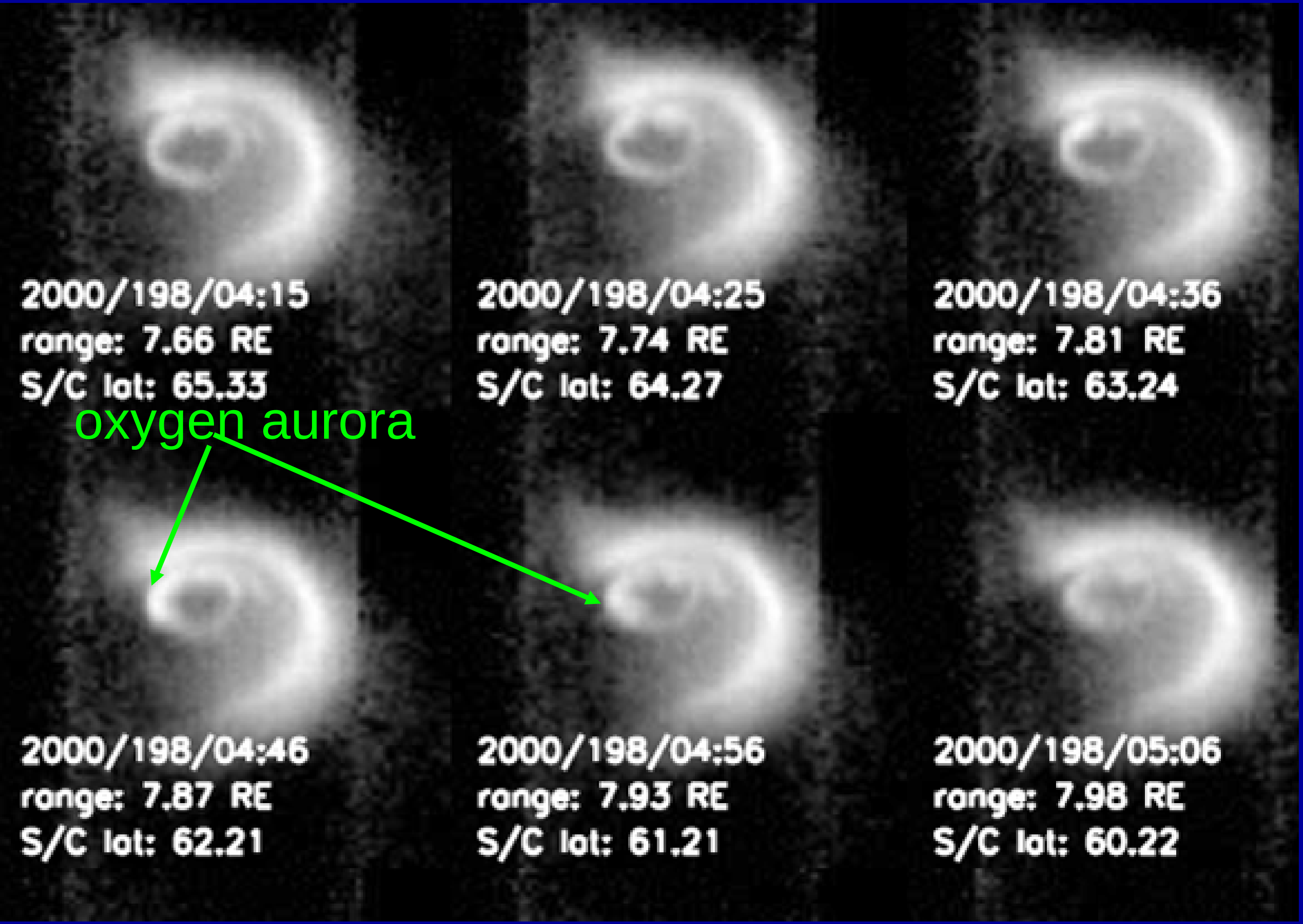

IMAGE/EUV sensor has residual sensitivity to O+ 53.9 nm emission.

NH pass shows bright feature at ~ L=3-4

Timing in qualitative agreement with ARGOS observations in SH

Stephan et al., JGR, 109, A09208, doi:10.1029/2004JA010557, 2004

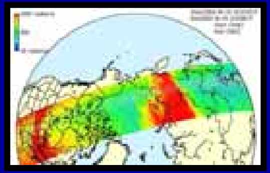

TIMED observes emissions consistent with mid-low latitude ENA/Ion auroras during all superstorms since 2002.

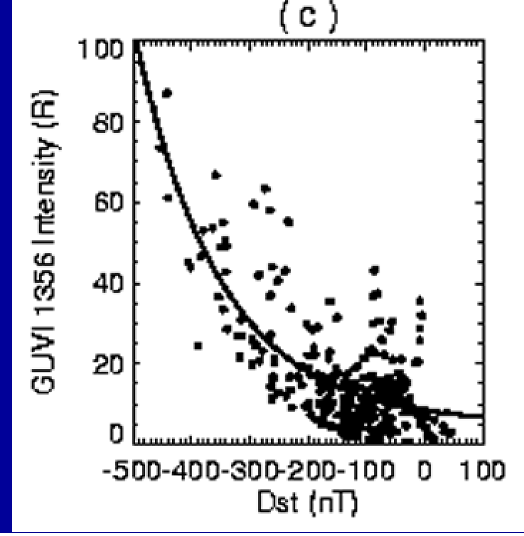

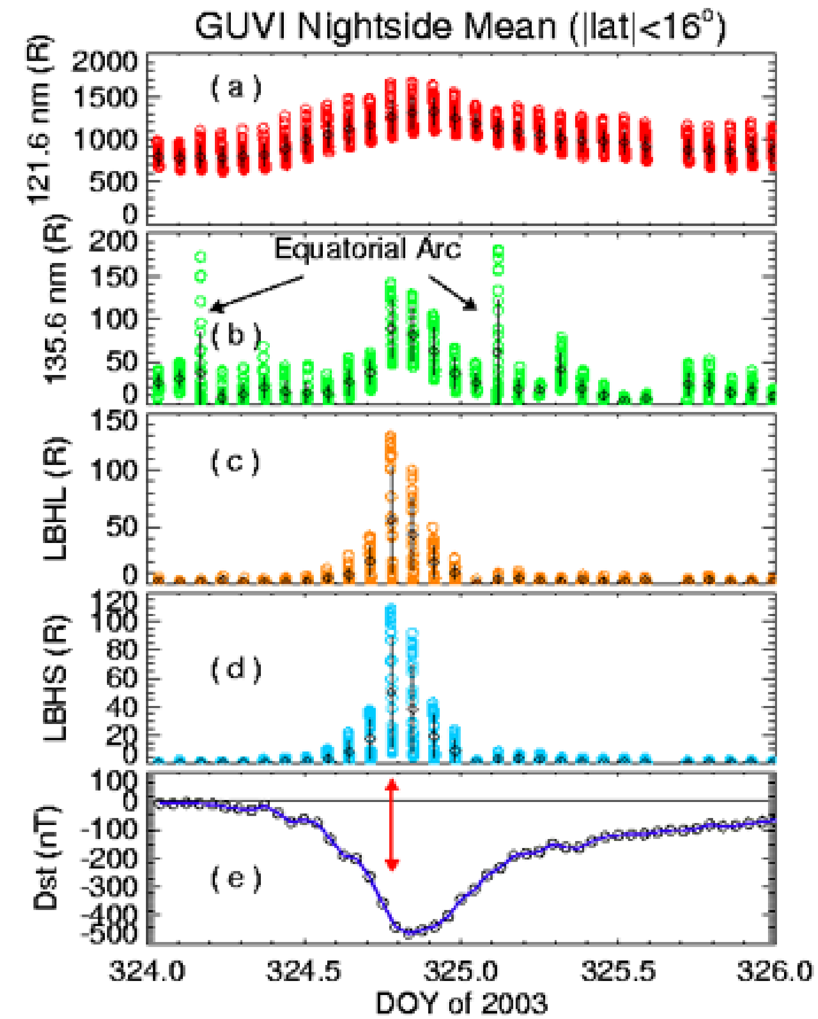

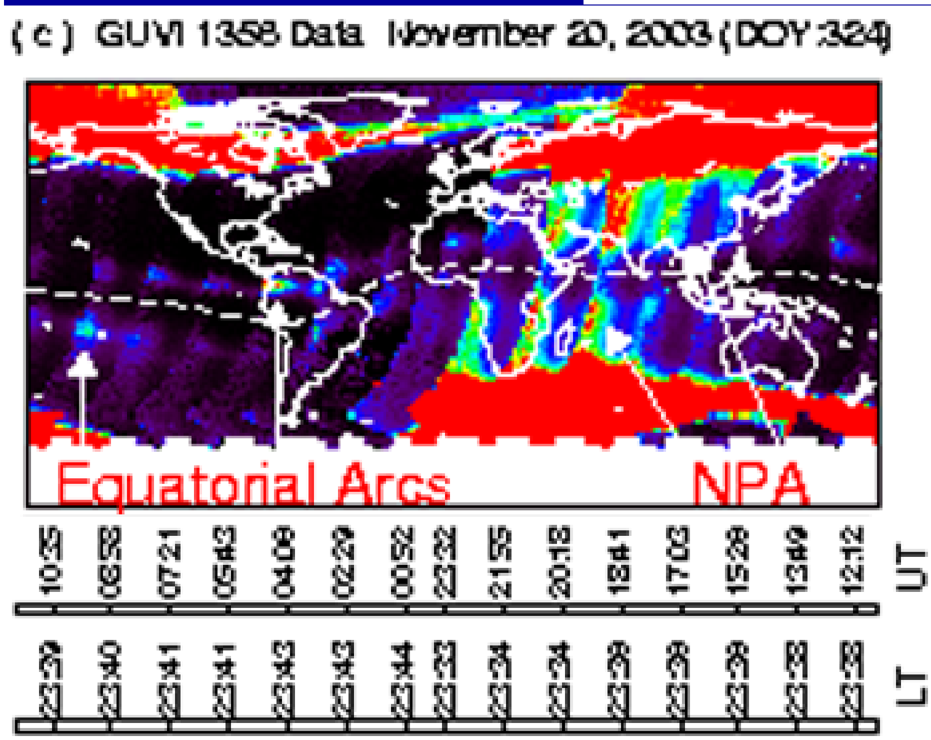

Zhang et al., submitted JGR, 2005

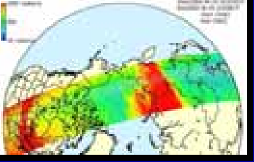

Ion auroras at midlatitudes

Soft ion and/or ring current ENA source?

Equatorial Anomolies (EA)

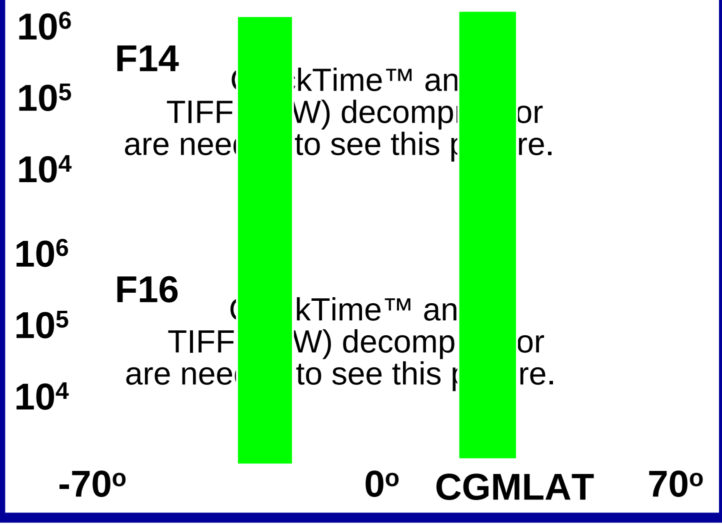

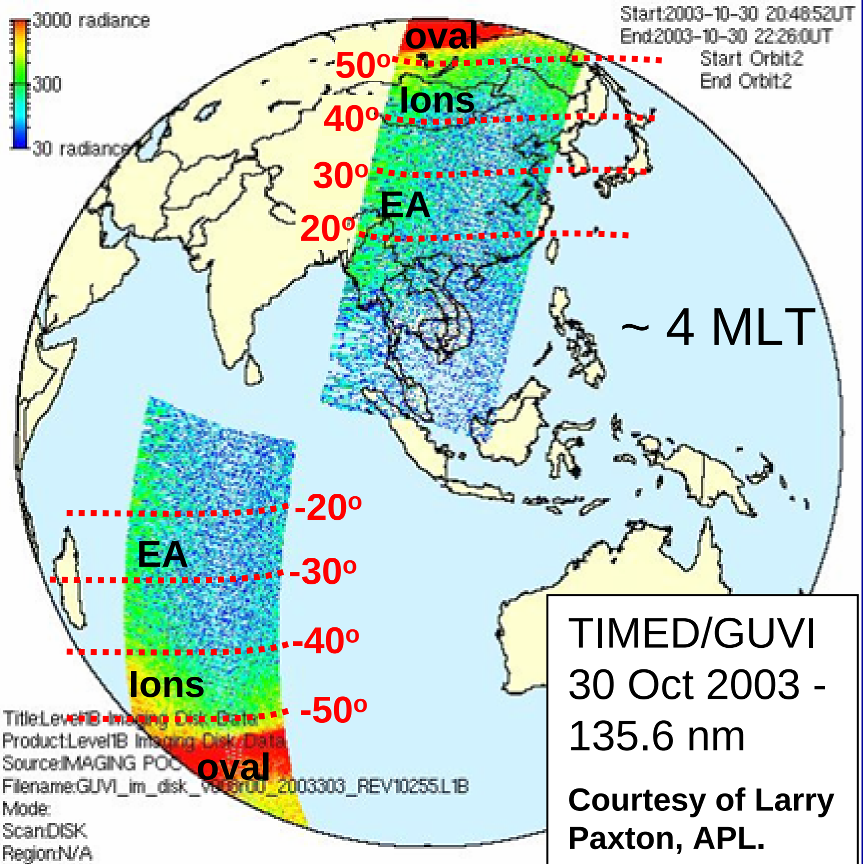

TIMED/GUVI 30 Oct 2003 - 135.6 nm

Courtesy of Larry Paxton, APL.

Soft Ion Source of Midlat Aurora

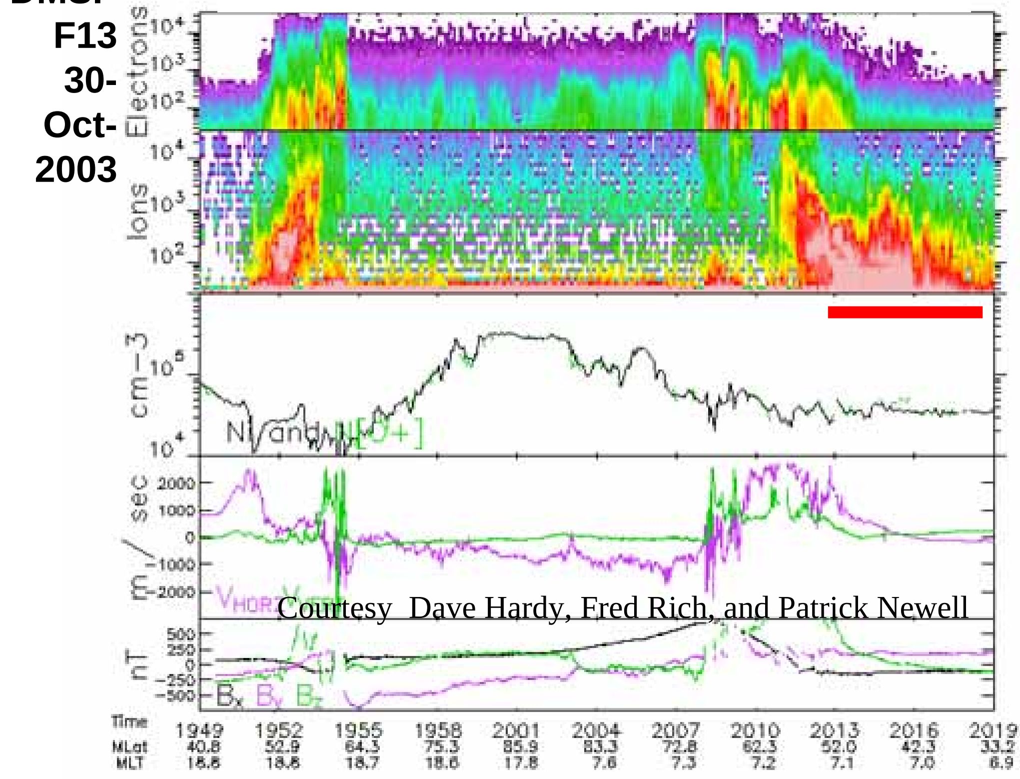

Courtesy Dave Hardy, Fred Rich, and Patrick Newell

SAR Arcs: Stable, long-lived, spectrally pure at 6300 Å, subauroral

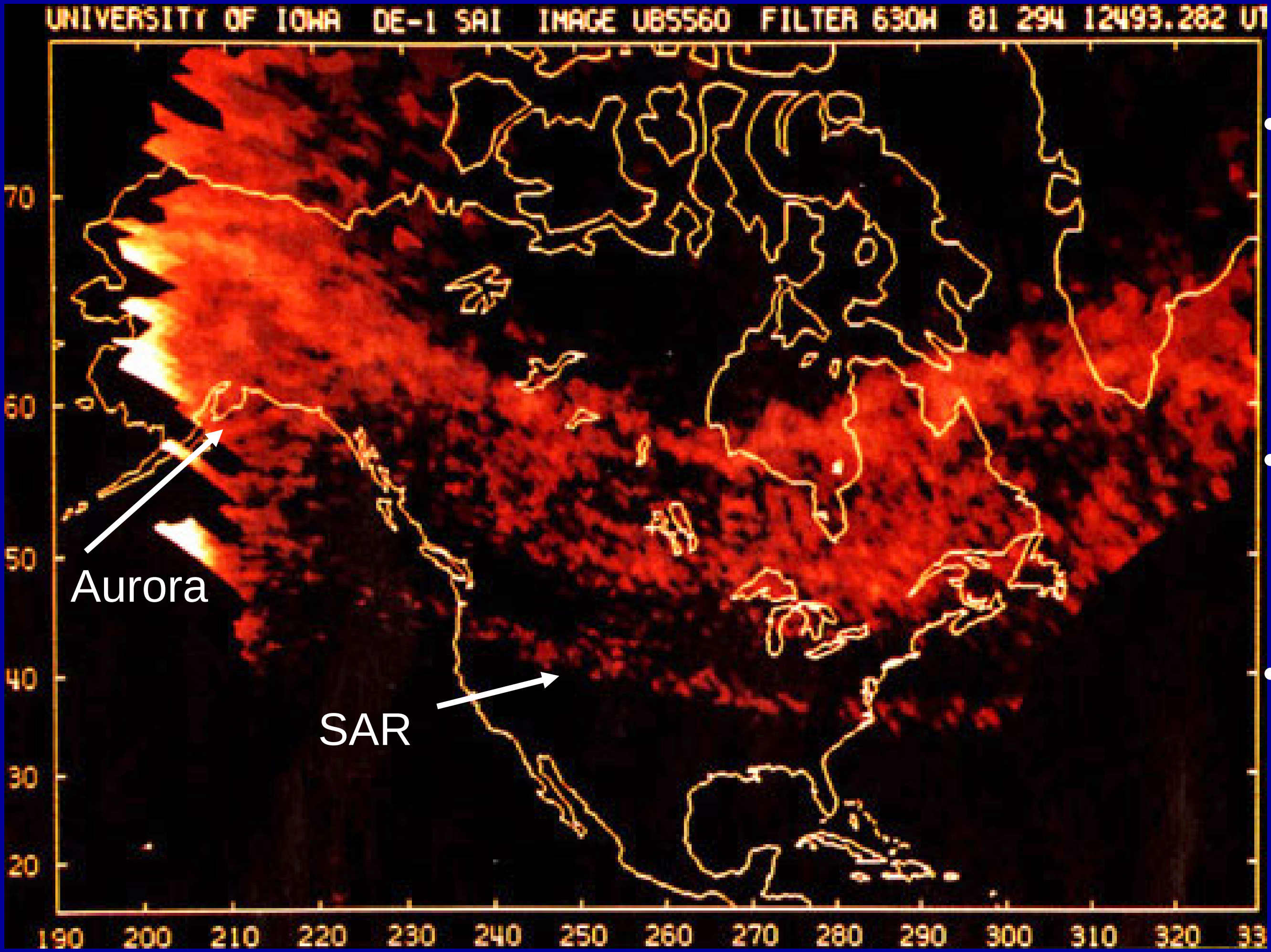

- Subvisual: Mean intensities 255 R (solar max), 111 R (solar min) [Slater & Kleckner 1989]
- Dayside weaker than nightside Te peaks [Kozyra et al., 1986]
- Soft electron precipitation (~1 eV flowing Maxwellian) [Gurgiolo et al., 1982]

Image : L. Frank and J. Craven from the Dynamics Explorer 1

Interaction of Different Ions with the Plasmasphere [c.f., Kozyra et al., Rev of Geophys., 1997]

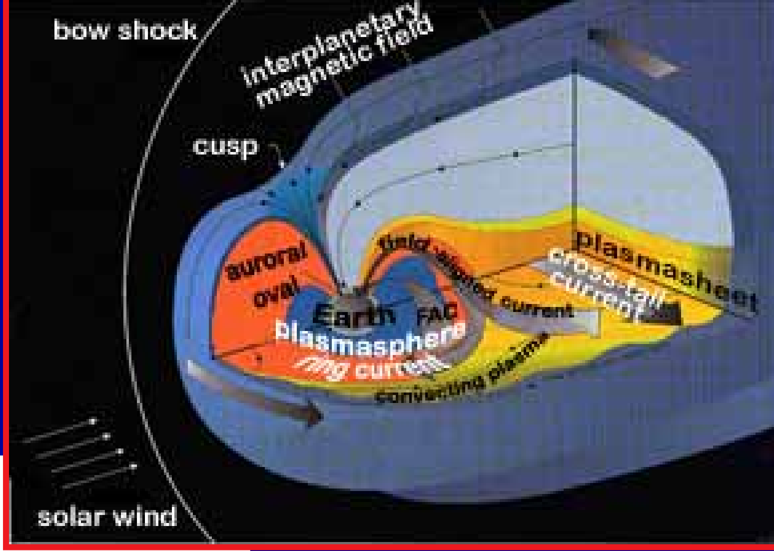

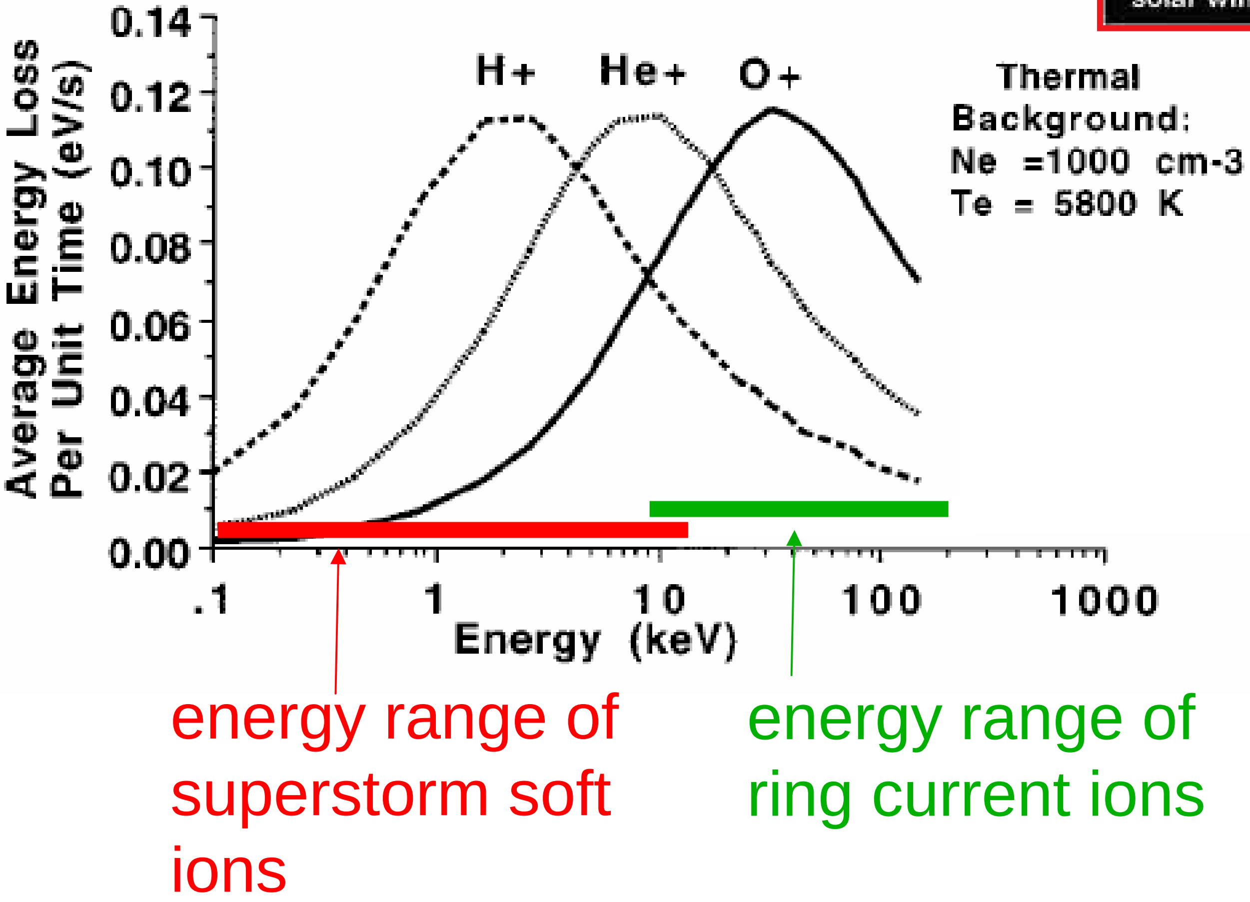

Note: A population of >10 keV H^+ ions overlapping the plasmasphere (as seen in superstorms) could also supply significant magnetospheric heat flux

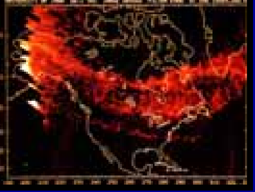

New Features of SAR Arcs during extreme events

- Subauroral Te peak reaches 10,000K
- Dawnside peak can be enhanced first and be stronger than duskside peak
- Strong soft (<10 keV) ion precipitation
    - •Coincident with Te peak.
    - •Broader MLAT extent & intensity on dawnside
    - •Appropriate energy & intensity to produce strong electron heating in plasmasphere

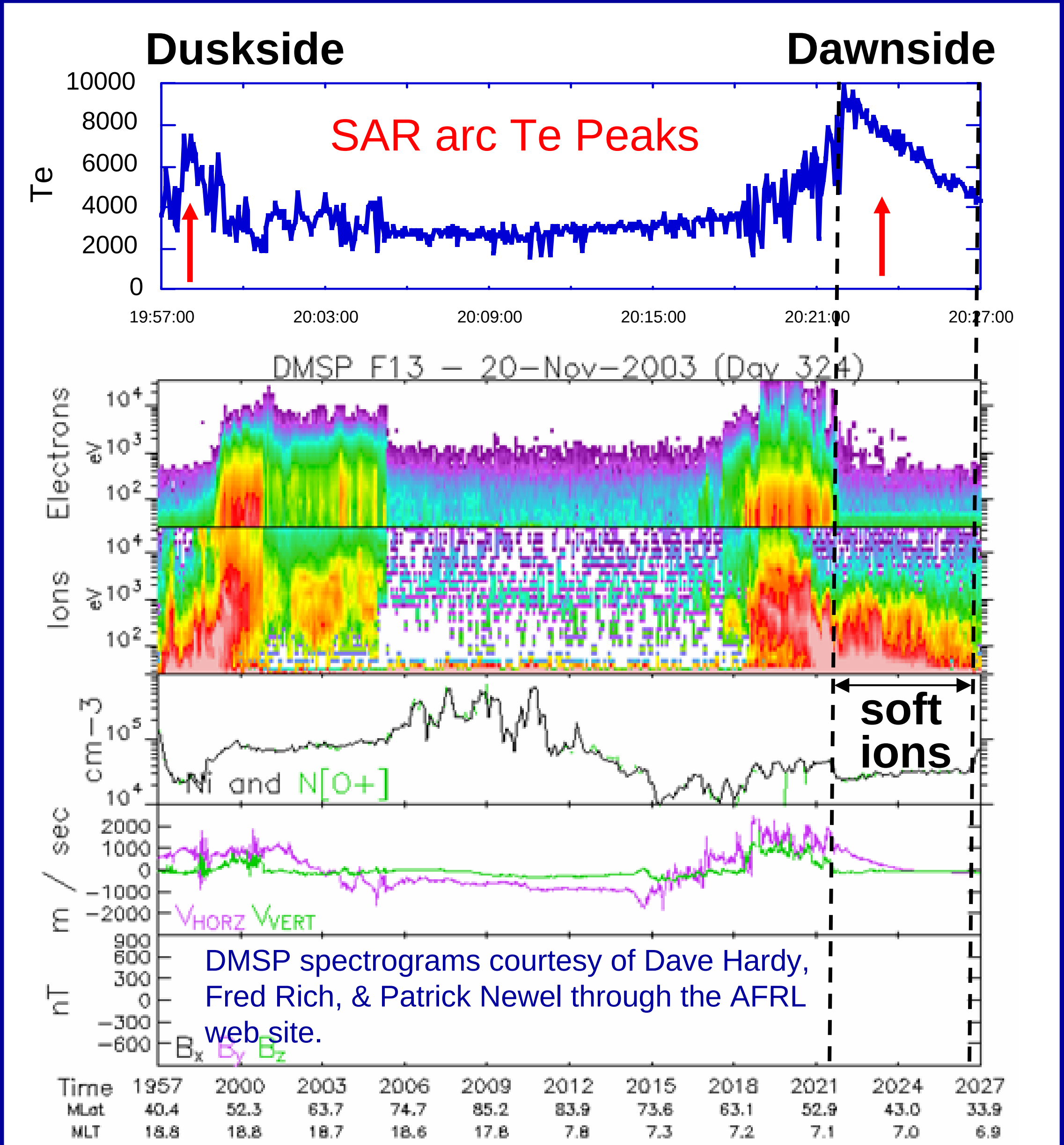

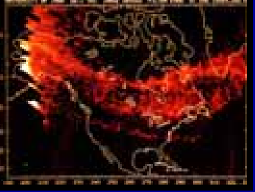

SAR Arcs are driven into visible range in superstorms

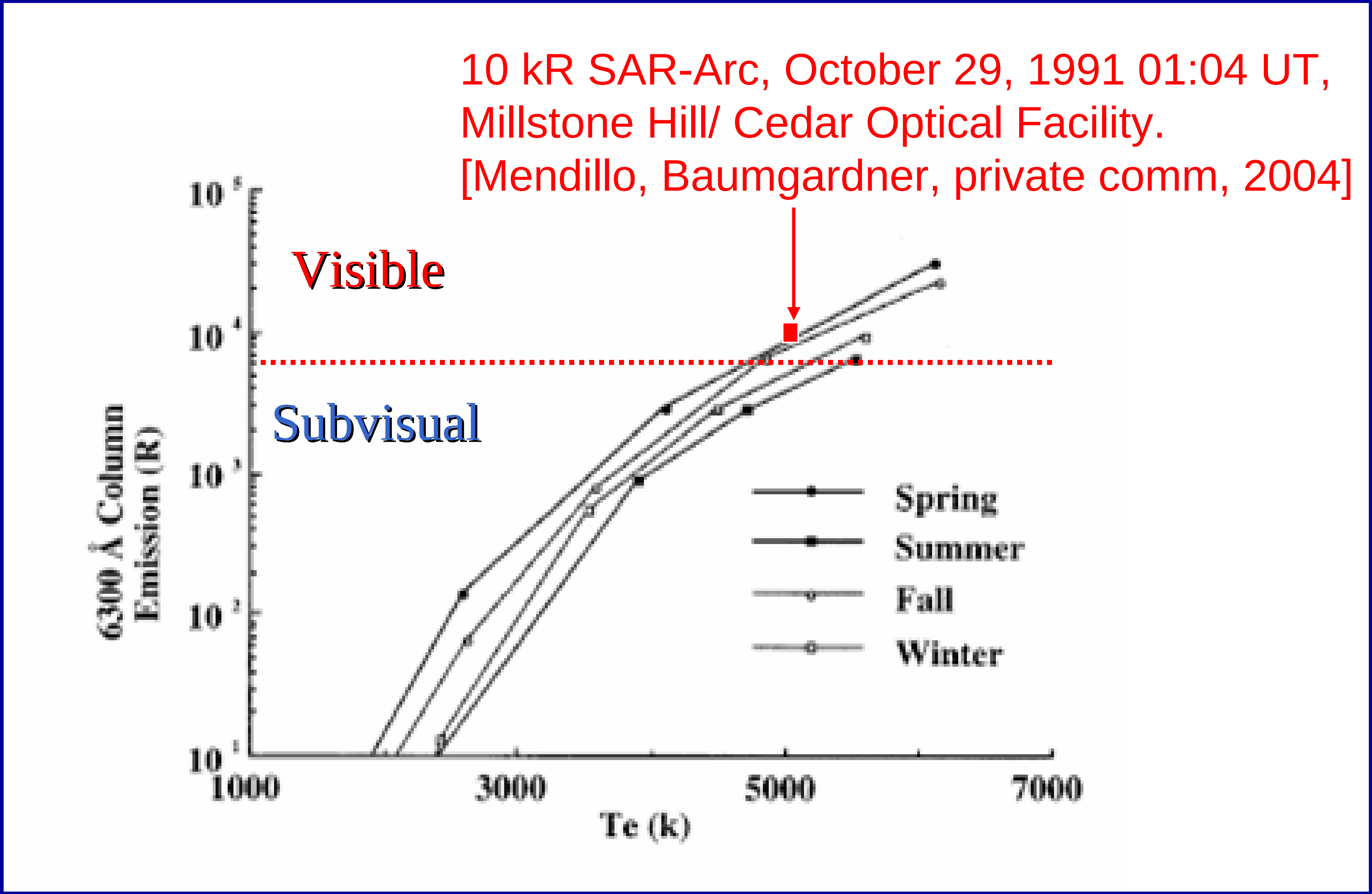

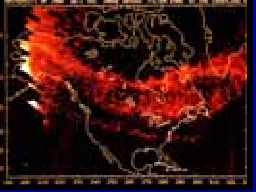

Strong Te Peaks 20-21 Nov 2003 Superstorm

[Courtesy R. Heelis, UT Dallas]

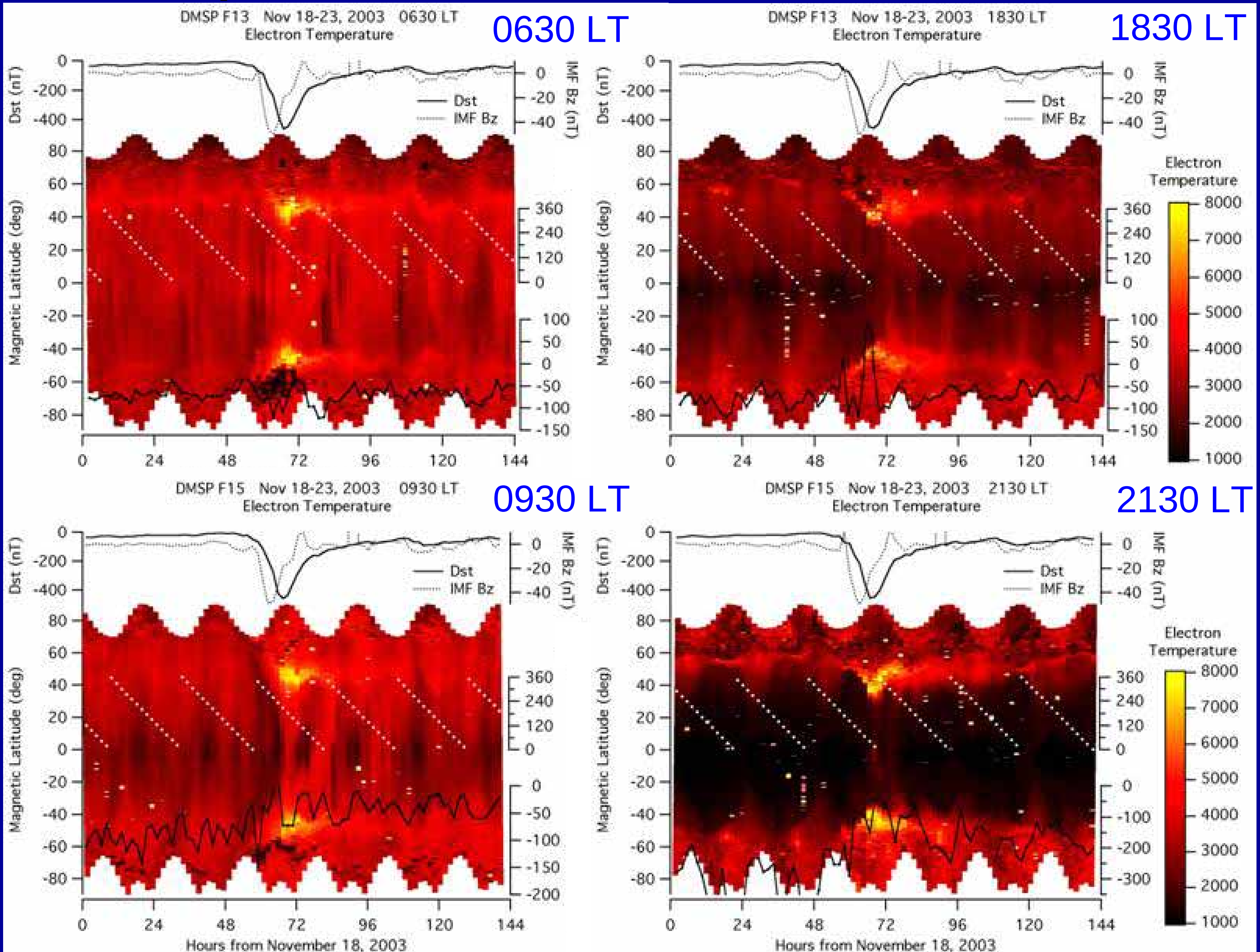

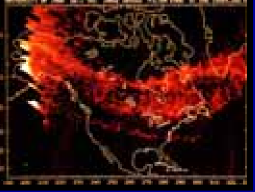

Strong Te Peaks 29-31 Oct 2003 Superstorm

[Courtesy R. Heelis, UT Dallas]]

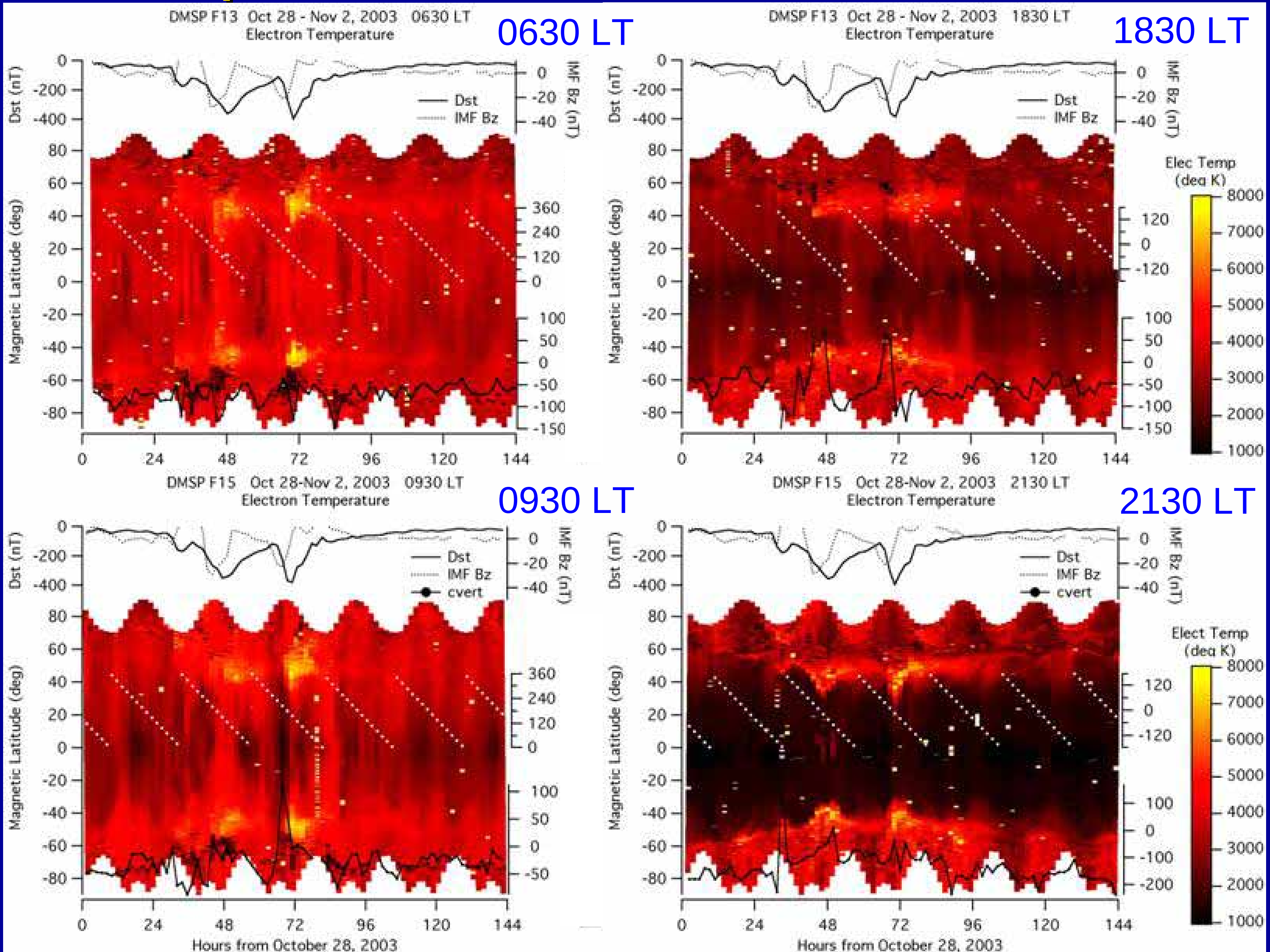

Summary

- Coulomb collisions, charge exchange, wave-particle interactions and scattering in stretched magnetic fields drive Particle and heat fluxes into the subauroral & low latitude ionosphere
- Effects on the ionosphere/atomosphere vary with precipitating ion species.
- New Observations are expanding our view of the impacts of subauroral heat and particle fluxes and their variation with activity:
  - Detached proton arcs give evidence that wave-particle interactions are occurring in regions that map to the subauroral ionosphere
  - First observations of the global extent of strong ion/atom auroras are being made.
    - Must have an impact on mid-low latitude ionospheric conductance, neutral heating, etc. Needs further investigation
    - Changes dynamically during the event
    - Feeds into electrodynamics of penetration and SAPs electric fields
  - SAR arc morphology in MLT and strength are altered during superstorms. Emissions are driven into the visible range associated with a new population of precipitating soft ions. Question remains: How is this related to great red auroras during superstorms?